SLAC-PUB-1473
CALT 68-441
August 1974
T/E

Scaling Laws for Large Momentum Transfer Processes*

STANLEY J. BRODSKY

Stanford Linear Accelerator Center, Stanford University, Stanford, California 94305

and

GLENNYS R. FARRAR

California Institute of Technology, Pasadena, California 91109

ABSTRACT

Dimensional scaling laws are developed as an approach to understanding the energy dependence of high energy scattering processes at fixed center-of-mass angle. Given a reasonable assumption on the short distance behavior of bound states, and the absence of an internal mass scale, we show that at large s and t, $d\sigma/dt\ (AB \to CD) \sim s^{-n+2} f(t/s)$; n is the total number of fields in A,B,C and D which carry a finite fraction of the momentum. A similar scaling law is obtained for large $p_\perp$ inclusive scattering. When the quark model is used to specify n, we find good agreement with experiments. For instance, this accounts naturally for the $(q^2)^{-2}$ asymptotic behavior of the proton form factor. We examine in detail the field theoretic foundations of the scaling laws and the assumption which needs to be made about the short distance and infrared behavior of a bound state.

(Submitted to Phys. Rev.)

*Work supported in part by the U. S. Atomic Energy Commission. Prepared under Contract AT(11-1)-68 for the San Francisco Operations Office, U. S. Atomic Energy Commission.

I. Introduction

The dimensional scaling laws[1,2]

$$\frac{d\sigma}{dt}\,(AB \to CD) \sim s^{-n+2} f(t/s) \tag{1}$$

for the asymptotic behavior of fixed angle scattering appear to compactly summarize the results of a broad range of hadronic scattering, photoproduction, and elastic form factor measurements. The integer n is given by the (minimum) total number of lepton, photon, and elementary quark fields carrying a finite fraction of the momentum in the particles A, B, C and D. The scaling laws represent, in the simplest possible manner, the connection between the degree of complexity of a hadron and its dynamical behavior.

One of the most important consequences of Eq. (1) is its application to elastic electron-hadron scattering. This rule immediately connects the aymptotic dependence of the (spin-averaged) electromagnetic form factor to the minimum numbers of fields n_H in the hadron:

$$F_H(t) \sim t^{1-n_H} \tag{2}$$

Thus, using the quark model, we have $F(t) \sim t^{-1}$ for mesons and $F_1(t) \sim t^{-2}$ for baryons. We also find (see Sec. II.B2) $F_2 \sim t^{-3}$, and thus $G_E \sim G_M$ scaling. All of these results are consistent with the asymptotic dependence indicated by present experiments. In Section III of this article we survey present data which is relevant to testing the scaling law, Eq. (1). It fares very well, being consistent in all cases and accurately verified for $\gamma p \to \pi p$ and $pp \to pp$. We predict $d\sigma/dt \to s^{-7}$ and s^{-10}, respectively, at fixed cm angle; experiment gives $s^{-7.3 \pm 0.4}$ and $s^{-9.7 \pm 0.3}$. A catalog of predictions which can be tested in the future is also given in Section III.

In fact, dimensional analysis and some simple assumptions immediately lead to the scaling law of Eq. (1). Imagine that a hadron is a bound state of n_H constituents each of which carries a finite fraction of the total hadron momentum. The amplitude for the scattering of a system of hadrons (see Fig. 1.) is therefore related to the amplitude for the scattering of their constituents, integrated over possible constituent momenta with the constraint that the constituent momenta add up to the hadron momenta. If the total number of fields in the initial and final states is n, the Feynman amplitude M_n has dimension $[\text{length}]^{n-4}$ when the conventional normalization of states is chosen $\left(\langle p | p' \rangle = 2E\delta^3(\underset{\sim}{p}-\underset{\sim}{p}')\right)$. If at large energy and momentum transfer $\sqrt{s}^{-1}$ is the only length scale for the amplitude, $M_n \sim (\sqrt{s})^{4-n} f(t/s)$. Now if each of the n_H constituents of hadron H carries a finite fraction of the momentum, say in the hadron rest frame, integrating over the possible momenta of the constituents can never introduce a dependence on s. Thus the amplitude, M, for the physical process has the same asymptotic behavior as M_n. Equation 1 then follows immediately since

$$\frac{d\sigma}{dt} \sim \frac{1}{s^2} |M|^2 \quad .$$

More generally for any exclusive process $A + B \to H_1 + \dots H_M$,

$$\frac{d\sigma}{dt_1 (d^3p_2/E_2) \dots (d^3p_{m-1}/E_{m-1})} \sim s^{-n+2} f\left(\frac{p_i \cdot p_j}{s}\right) \tag{3}$$

for large s at fixed invariant ratios. Alternatively, using the quark model we have simply the scaling law

$$\Delta\sigma \sim s^{-1-N_M-2N_B} \tag{4}$$

for the exclusive cross section integrated over any fixed center-of-mass region when the ratios of invariants stay finite. Here $N_M(N_B)$ is the total number of mesons (baryons) in the initial and final state.

The same model and dimensional counting rules may be applied to inclusive processes $A + B \to C + X$ where C is detected at large transverse momentum[1]. In this case only a subset N of the constituent fields need to participate in the large angle scattering process; the rest remain as "spectators". The result for $s \gg M^2$, fixed invariant ratios, is

$$\frac{d\sigma}{d^3p/E} = \frac{1}{s^{N-2}} f\left(\frac{t}{s}, \frac{M^2}{s}\right) = \frac{1}{\left(p_\perp^2\right)^{N-2}} \tilde{f}\left(\theta_{cm}, \frac{p_{cm}}{p_{max}}\right) \tag{5}$$

where M^2 is the missing mass. The subset N which contributes to the scaling of a given hadronic process can be model dependent; we discuss this further in Section IV. Furthermore, as shown in Ref. 3, the dimensional rule allows one to predict the threshold dependence at the exclusive boundary (i.e., $\frac{M^2}{s} = (1 - \frac{p_{cm}}{p_{max}}) \to 0$ at fixed θ_{cm}):

$$\frac{d\sigma}{d^3p/E} \sim \frac{1}{s^{N-2}} \left(\frac{M^2}{s}\right)^P \quad , \; P = 2\tilde{n} - 1 \tag{6}$$

where $\tilde{n}$ is the total number of spectators in A, B, and C. Thus for example in deep inelastic e-p scattering $N = 4$ (for $eq \to eq$) and $\tilde{n} = 2$ (for the two spectator quarks in the proton) and we recover both scale-invariance for νW_2 and the Drell-Yan-West behavior $\nu W_2 \sim (1-x)^3$ for $x \to 1$. Possible spin modifications are reviewed by Ezawa, Ref. 4. As shown in Ref. 1, the inclusive-exclusive connection of Bjorken gives the relation $n = N + P + 1$, where n is the number of fields involved in the exclusive scattering (see Eq. 3).

The above scaling laws share a significant feature with the predictions of parton models: the cross section multiplied by a power of s becomes a universal scale-independent function, dependent only on ratios of invariants. In contrast, if hadrons were homogeneous objects, no elementary constituent would carry a finite fraction of the total momentum, and large transverse momentum hadron scattering would take place via the cumulative effect of an infinite number of soft interactions. Exponential damping in transverse momentum is therefore to be expected in such a model[5].

It is evident that more careful reasoning is necessary in order to establish that Eqs. (1 - 5) should be true. That is the purpose of Section II of this article. The principle issue of course is whether masses or binding energies could set the scale rather than s. In the deep inelastic case that seems not to happen when q^2 and ν become sufficiently large. We argue in Section II that for exclusive scattering when all kinematic variables are large it is likely that again only those large invariants set the scale. Of course purely dimensional reasoning cannot specify possible powers of logarithms. Hence all the scaling laws discussed above must be regarded by the reader as true "modulo logs." In Section II our analysis of renormalizable field theories will allow us to be more precise about logarithmic modifications to canonical power-law scaling.

The simple model of the hadron in which its momentum is partitioned among its constituents so that each quark has a finite fraction turns out to be very useful for a broad range of hadronic scattering calculations - especially those involving multiquark states. An application to effective Regge trajectories and residue functions is given in Section II.B2. Section III is devoted to the experimental situation and Section IV briefly deals with inclusive reaction applications. Appendix A gives a detailed example of a Born amplitude calculation. Finally Appendix B shows that the fixed angle unitarity bound on the asymptotic behavior of scattering amplitudes is the same as the dimensional scaling law $|M_n|^2 \sim s^{4-n}$.

II. Exclusive Scaling Laws.

The crucial steps in the dimensional analysis of the scaling laws given in the introduction are a) the effective replacement of the composite hadron by constituents carrying finite fractions of the hadronic momentum, and b) the absence of any mass scale in the amplitude M_n or binding corrections to it. It is evident that a super- or a non-renormalizable field theory could not satisfy these conditions since such theories contain a fundamental length (in the coupling constant) which necessarily sets the scale. This is in contrast to renormalizable perturbation theories in which mass scales enter through propagators and external masses. In fact the required conditions a) and b) are natural features of renormalizable field theories given certain dynamical assumptions concerning the nature of the Bethe-Salpeter wave function, the absence of infrared effects, and the accumulation of logarithms.

In this section we shall systematically investigate the validity in renormalizable field theories of the dimensional argument and its underlying assumptions. In order to examine the effects of binding in bound state scattering (a), we shall use the Bethe-Salpeter formalism[6]. This enables one to separate the behavior of individual graphs from that due to the infinite summation required to form bound states. By definition the hadronic amplitude is given by the convolution of the hadronic wave functions and an n-particle amplitude M_n integrated over relative momenta $k^\mu{}_i$ (see Fig. 2).

$$M = \int \psi^+_{BS} \, \psi^+_{BS} \, M_n \, \psi_{BS} \, \psi_{BS} \prod_i d^4k_i \; . \tag{15}$$

We shall discuss b), the asymptotic behavior of M_n, by explicitly examining it in perturbation theory. We shall show that with the following three assumptions, the scaling laws (Eqs. 1-4) are correct (modulo logarithms) in any renormalizable field theory:

A) The physical mesons and baryons are s-wave Bethe-Salpeter bound states of quark-antiquark and three quark fields respectively, such that the wave functions are finite when the quarks have zero separation in coordinate space and vanish for large coordinate separation. Thus the large momentum components of the wave function are restricted: e.g., for the mesons we have

$$\int d^4k\ \psi_M(k) = \psi_M(x_\mu=0) < \infty \quad . \tag{8}$$

Moreover, since the coordinate space extent of the wave function is bounded, the wave function is finite at every point in momentum space.

B) The large momentum transfer interactions of the constituents are asymptotically scale invariant.

C) Multiple ($L \geq 2$) scale-invariant interactions between the constituents of different hadrons can be neglected.

Assumption A is necessary so that binding corrections are limited. Then the computation of M_n involves the scattering amplitude obtained by replacing each hadron by a collection of quarks of the appropriate spin, each constituent carrying a finite fraction of the hadron's momentum. Note that if we turn off the binding adiabatically, the constituent momenta are $p_i = (m_i,\vec{0})$ in the rest system and $p_i = x_i p_H$, $x_i = m_i/m_H$ in a general frame. Assumption A implies that there are no elementary fields with the quantum numbers of the hadrons. Because of assumption A, the d^4k_i integrations are convergent in Eq. (7), and it is easy to see that the scaling behavior at fixed angle of M is given by the scaling behavior of M_n multiplied by finite coefficients of order $\psi(x=0)$. Note that in the case of non-zero orbital angular momentum, helicity constraints, or quantum number restrictions, the amplitude M could fall by additional powers of s.

Assumptions B and C are necessary to insure that $M_n \sim (\sqrt{s})^{4-n}$. Assumption C serves to eliminate asymptotic contributions to M_n from disconnected graphs (see Fig. 3). Recently Landshoff[7] has made the important observation that $M_n \not\sim (\sqrt{s})^{4-n}$ if hadrons can scatter at large angles by successive independent, near mass shell elastic scatterings of each constituent of one off a constituent of the other (as in Fig. 3). In fact (see Sec. II.B1 and Appendix A) in this case $M_n \sim (\sqrt{s})^{4-n} \cdot (\sqrt{s})^{L-1}$ where L is the number of pairs of constituents from different hadrons which have a large angle scale invariant interaction. (It should be noted that whether or not this process takes place in hadron-hadron scattering, there is no modification from such a phenomenon to form factors or to fixed angle processes involving photons or leptons.) However, there is both direct and indirect evidence that Landshoff's mechanism is not physically important at least at present energies. The direct evidence is that in $pp \to pp$, $d\sigma/dt \sim s^{-9.7 \pm 0.3} f(t/s)^8$ rather than the s^{-8} as would be predicted if L=3. More indirect but equally important is the fact that no high energy, fixed angle scale invariant interaction between quarks of different hadrons seems to occur in nature. The best evidence of this is from high $p_\perp$ inclusive pion production ($pp \to \pi + X$) whose cross section falls much faster than the $p_\perp^{-4}$ at fixed $p_\perp/\sqrt{s}$ predicted if such a scale invariant interaction between quarks of different hadrons did occur (see Section IV for details). For these empirical reasons, then, assumption C is necessary.

The organization of this section is as follows. We proceed by first (Section II.A) giving the construction of an amplitude in terms of Bethe-Salpeter wave functions in the spinless constituent case, using the meson form factor as an example (II.A1). We show that with assumption A the asymptotic behavior of the full amplitude is the same as the behavior of the dominant irreducible contribution, M_n. The extension of the analysis to spin-1/2 constituents is not difficult and is given in Section II.A2. We show that the meson form factor has the same behavior in the spin-1/2 as in the spinless case. This is an appropriate point to explain why, even though short distances are being probed, bound states of spin-0 fields (whose dimension is $[L]^{-1}$) and spin-1/2 fields (dimension $[L]^{-3/2}$) have the same behavior in large momentum transfer exclusive scattering. In Section II.A3 we confront the difficult question of the validity of our assumptions A and B. Not very much is known about the short distance and infrared behavior of Bethe-Salpeter wave functions. We review what is known, give some plausibibity arguments in favor of our assumptions, and speculate on the situation in non-abelian gauge theories. Modifications in our results when the wave function at short distances is not finite are discussed.

Having established that assumption A reduces the problem to the behavior of irreducible graphs, we examine the lowest order irreducible (Born) graphs for a number of interesting processes in Section II.B. We start (II.B1) with the Landshoff diagrams and show why they violate the dimensional result. We present some speculative arguments in favor of assumption C, which allows us to neglect their contribution. Next (II.B2) we show that the behavior of the connected Born diagrams reproduces our scaling law independent of the spin of the constituents or the details of the interaction as long as the coupling constants are dimensionless. While discussing the Born diagrams we show that a model with spin-1/2 quarks gives G_E/G_M asymptotic scaling. We also obtain from general arguments the asymptotic Regge trajectories in gluon exchange and quark interchange models. Finally, in Section II.B3 we discuss the effects of higher order corrections to the Born diagrams.

II.A1 Spinless Bethe-Salpeter Wave Function and the Meson Form Factor.

The simplest example, which illustrates how to obtain the asymptotic behavior of an hadronic amplitude is the calculation of the form factor of a meson, taken as a bound state of two scalar fields. The full Bethe-Salpeter wave function satisfies[6] (see Fig. 4)

$$(k^2-m_a^2)((p-k)^2-m_b^2)\psi_p(k) = \int \frac{id^4\ell}{(2\pi)^4} K(k,\ell,p)\psi_p(\ell) \quad . \tag{9}$$

(Note that the wave function Ψ, as conventionally defined, includes the propagators for the constituent legs.) This is the eigenvalue equation for the meson mass $M^2 = p^2$. The kernel $K(k,\ell,p)$ is the sum of all two particle irreducible diagrams. For illustration we first consider a generalized ladder approximation

$$K_L(p,k,\ell) = g^2 \int \frac{\sigma(\lambda^2)\,d\lambda^2}{(\ell-k)^2 - \lambda^2 + i\varepsilon}$$

where we can choose the spectral function $\sigma(\lambda^2)$ such that for large ℓ^2, $K_L(p,k,\ell)$ scales as $(\ell^2)^{-\delta}$. For a super-renormalizable theory δ is positive; ϕ^3 theory corresponds to $\delta = 1$. For renormalizable theories, e.g., ϕ^4, $\delta = 0$. We shall always compute with $\delta > 0$ as a regulator, and take the limit $\delta \to 0$ at the end of the calculation[9]. This is analogous to the generalized Feynman Pauli-Villars method or dimensional regularization in perturbation theory. Note that for $\delta > 0$, we have $\psi_p(k) \sim [k]^{-4-\delta}$ and $\psi_p(x=0) < \infty$. (The minimum condition for $\psi_p(x=0) < \infty$ is $\psi_p(k) \sim [k]^{-4}/[\log(k^2)]^{1+\varepsilon}$ with $\varepsilon > 0$.)

The form factor in ladder approximation is (see Fig. 5)

$$(2p+q)^\mu F(q^2) = \langle p+q|J^\mu(0)|p\rangle$$

$$= \int \frac{i d^4k}{(2\pi)^4} \psi^\dagger_{p+q}(k)(2k+q)^\mu[(p-k)^2 - m_b{}^2]\psi_p(k) + (a \leftrightarrow b), \quad (10)$$

If additional kernals are introduced which contain internal charged lines, then additional contributions to the current in Eq. (10) are obtained consistent with gauge-invariance. A comprehensive treatment of these contributions has been given by Mandelstam[6]. The loop corrections are non-leading for $q^2 \to \infty$ if $\delta > 0$, and can give logarithmic corrections for each loop as $\delta \to 0$. We return to their contributions below.

By assumption A the wave functions are bounded at every point in momentum space, so that the asymptotic behavior of $F(q^2)$ is controlled by two regions of the d^4k integration:

(a) $k \sim xp$; $k^2 \sim 0(m^2)$, $(p-k)^2 \sim 0(m^2)$, $(k+q)^2 \sim (1-x)q^2$,

(b) $(k+q) \sim x(p+q)$; $(k+q)^2 \sim 0(m^2)$, $(p-k)^2 \sim 0(m^2)$, $k^2 \sim (1-x)q^2$

where x is finite. More precisely, integration region (a) corresponds to $k = xp+\kappa$, where κ is a spacelike vector orthogonal to p which is of bounded magnitude (by assumption A that the wave function is damped in large relative momenta). Thus $k^2 = x^2m^2 + \kappa^2$ and $k \cdot p = xm^2$ are finite. (The variable x is similar to the variable used in the Sudakov and infinite momentum frame analyses.) It is easily shown that, after the dk^2 integration is done, only the region $0 \leq x \leq 1$ can contribute. Region (b) corresponds to $k = (p+q) + \kappa'$ with $\kappa' \cdot (p+q) = 0$ and (κ'^2) bounded.

At this point we can relate the asymptotic fall-off of $F(q^2)$ to that of $q^2\psi(q^2)$, up to logarithms. However, for our purposes it will be convenient to iterate the equation of motion wherever large relative momentum is encountered. Thus we obtain for large q^2

$$(2p+q)^\mu F(q^2) \cong \int \frac{id^4k}{(2\pi)^4} \int \frac{id^4\ell}{(2\pi)^4} \psi^\dagger_{p+q}(\ell) M^\mu_5(p,q,\ell,k)\psi_p(k) \tag{11}$$

with $k = xp + \kappa$ and $\ell = yp + \kappa'$, The integrations are limited to the dominant region of each wavefunction: κ^2 and $\kappa'^2 = 0(m^2)$. M^μ_5 is the five-point connected scattering amplitude illustrated in Fig. 6.

This is in fact the prototype of our general procedure. We employ the equation of motion for the wave function wherever it involves large relative momentum. In this manner we generate the connected amplitude M^μ_5 which represents the scattering of the quark constituents, each with a finite fraction of the hadron momenta: $P_i = x_i P_H$, $\sum_i x_i = 1$. M^μ_5 is of course exactly the connected amplitude which occurs when the hadronic binding is turned off adiabatically, in which case $x_i \to m_i/M_H$.

Let us now discuss the asymptotic behavior of $F(q^2)$ using Eq. (11). For large q^2 one can readily verify that

$$M^\mu_5 \sim \frac{(2xp+q)^\mu}{(1-x)q^2} \frac{1}{[(1-y)q^2-(x-y)q^2]^\delta} + \frac{2y(p+q)^\mu - q^\mu}{(1-y)q^2} \frac{1}{[(1-y)q^2-(x-y)q^2]^\delta}$$

which is properly gauge invariant: $q_\mu M^\mu_5 = 0$. Asymptotically, then,

$$F(q^2) \sim \left(\frac{1}{q^2}\right)^{1+\delta} \log q^2/m^2$$

where the logarithm occurs because of the endpoint of the integration over $(1-x)^{-1}$ or $(1-y)^{-1}$. This result for $\delta > 0$ agrees with those of Ref. 9.

More generally the higher order kernels modify this result by extra powers of $(q^2)^{-\delta}$ for $\delta > 0$, and by possible logarithms for each additional loop if $\delta = 0$. However, if we assume that the true ultraviolet behavior of the theory is more convergent than indicated by elementary gluon exchange (as in asymptotically free theories, for example), then the proper regularization of the renormalizable theory is $\delta = 0^+$ and additional logarithmic modifications are suppressed. This is a consequence of our assumptions A and B, that the accumulation of logarithms affects neither the asymptotic behavior of the wavefunction nor the scale invariance of the connected amplitude M_5^μ. We thus have the prediction for a bound state of two spin-0 particles :

$$F(q^2) \sim \frac{1}{q^2} \log q^2/m^2 .$$

In the case of an n-field bound state, we have simply (neglecting logs)

$$F(q^2) \to (q^2)^{1-n} \; (q^{2\delta})^{1-n} ,$$

i.e., $F(q^2) \sim (q^2)^{1-n}$ in the renormalizable limit in agreement with Eq (2). A detailed discussion of this result when n = 3 has been given by Alabiso and Schierholz[9]. Note that the powers of $(q^2)^{-1}$ arise from each off-shell constituent line and the $(q^2)^{-\delta}$ from each gluon line.

Thus, physically, one pays the penalty of one power of q^2 for changing the direction of each constituent from along p to along p+q. The spin independence of this result is discussed in the next section.

II.A2 Spin-1/2 Constituents.

The calculations of the asymptotic behavior of form factors become somewhat more complicated when the effects of spin are included. The results in the renormalizable limit, however, are effectively the same as the spinless results. We begin with the example of the form factor of a meson which is a bound state of two spin-1/2 fields. We assume, for the present, zero orbital angular momentum. The Bethe-Salpeter wave function satisfies (see Fig. 4)

$$(\not{k}-m_a)(\not{p}-\not{k}-m_b)\psi_p(k) = \int \frac{id^4\ell}{(2\pi)^4} K(k,\ell,p)\psi_p(\ell) \tag{12}$$

where K is the full Bethe-Salpeter two-particle irreducible kernel. Again, as in the spinless case, we begin with the generalized ladder approximation form

$$K_L(k,\ell,p) = g^2 \int d\lambda^2\, \sigma(\lambda^2)\, \frac{\Gamma_{(a)}\, \Gamma_{(b)}}{(k-\ell)^2 - \lambda^2 + i\varepsilon} \quad . \tag{13}$$

The $\Gamma_{(a)}$ and $\Gamma_{(b)}$ represent the (momentum-independent) Dirac couplings of the gluons to constituent a and b respectively. Just as in the spinless case, we may choose $\sigma(\lambda^2)$ such that $K_L(k^2) \sim (k^2)^{-1-\delta}(\delta > 0,\ k^2 \to \infty)$, which gives assumption A: $\psi(x=0) = \int d^4k\ \psi_p(k) < \infty$. Renormalizable theories correspond to $\delta \to 0^+$, at least in the ladder approximation. This is discussed further in Section II.A3.

The form factor for the bound state using the kernel (Eq. (13)) is

$$\begin{aligned} \langle p+q|J_\mu(0)|p\rangle &= (2p+q)_\mu F(q^2) \\ &= e_a \int \frac{id^4k}{(2\pi)^4} \psi^\dagger_{p+q}(k+q)\gamma_\mu^{(a)}(\not{p}-\not{k}-m_b)\psi_p(k) \\ &\quad + (a \leftrightarrow b) \quad . \end{aligned} \tag{14}$$

Additional contributions required by gauge-invariance are necessary in the presence of the higher loop kernels, as in the spinless case (see Fig. 6). These are of the same order or are non-leading for $q^2 \to \infty$ if $\delta > 0$.

As in the spinless calculation, the important contributions for the asymptotic form factor occur when only one of the two wave functions is evaluated at large relative momentum. Again, it is convenient to iterate the wavefunction at large relative momentum using the equation of motion and we obtain

$$(2p+q)^{\mu}F(q^2) \sim \int \frac{d^4k}{(2\pi)^4} \int \frac{d^4\ell}{(2\pi)^4} \ \bar{\psi}_{p+q}(\ell) M_5^{\mu} \psi_p(k) . \tag{15}$$

M_5^{μ} is the connected Feynman amplitude shown in Fig. 7. As in the spinless case the dominant contribution comes when the constituents carry finite fractions of the longitudinal momenta and small transverse momenta. Furthermore, if only the leading q^2 dependence of the form factor is desired, the spin structure of the wave function simplifies enormously. In general the structure is

$$\psi_p(k) = [f_{1a}(p,k)\not{k} + f_{2a}(p,k)m_a][f_{1b}(p,k)(-\not{p}+\not{k}) + f_{2b}(p,k)m_b] . \tag{16}$$

Using the identities

$$\frac{\not{k}+m}{2m} = \sum_{\text{spin}} u(k,s)\bar{u}(k,s)$$

and

$$\frac{-\not{k}+m}{2m} = - \sum_{\text{spin}} v(k,s)\bar{v}(k,s) ,$$

Eq. (16) can be rewritten[10] in the form

$$\psi_p(k) = \Big\{ u_a(k)\bar{v}_b(p-k)\psi_p^{+-}(k) + v_a(k)\bar{u}_b(p-k)\psi_p^{-+}(k)$$

$$+ u_a(k)\bar{u}_b(p-k)\psi_p^{++}(k) + v_a(k)\bar{v}_b(p-k)\psi_p^{--}(k)\Big\} \quad , \qquad (17)$$

with the appropriate spin projections understood. In the zero binding limit this structure must reduce to the product of two free spinors $u_a(k=xp)\bar{v}_b(p-k=(1-x)p)$, hence for our purposes we may use

$$\psi_p(k) \approx u_a(k)\bar{v}_b(p-k)\psi_p^{+-}(k). \qquad (18)$$

The terms thus neglected are at least linear in κ^μ, (the "transverse momentum" which cannot become large) and give a non-leading contribution to $F(q^2)$. That these terms are proportional to the binding energy and may be therefore legitimately neglected is easily seen[10] in time-ordered perturbation theory: they arise from the presence in the wave function of an extra $q\bar{q}$ pair.

With the simplification, Eq. (18), we find

$$(2p+q)^\mu F_\pi(q^2) \propto \int_{k\approx xp} d^4k \int_{\ell\approx y(p+q)} d^4\ell \;\; \psi_{p+q}^{+-\dagger}(\ell)\tilde{M}_5^\mu \;\; \psi_p^{+-}(k) \quad , \qquad (19)$$

where

$$\tilde{M}_5^\mu = \bar{u}_a[y(p+q)]v_b[(1-y)(p+q)]M_5^\mu(k=xp,\ell=y(p+q)) \; .$$

$$u_a[xp]\bar{v}_b[(1-x)p] \quad ,$$

is the connected amplitude evaluated between on-shell spinors. Again note that for the connected tree graph we can neglect the κ and κ' components of k^μ and ℓ^μ, and except for particular helicity configurations we may drop all mass terms in the asymptotic limit. This is explicitly evident in the Breit frame ($\vec{q}^{\,2} = -q^2$):

$$p = \left(\sqrt{m^2 + \vec{q}^{\,2}/4} \quad , \; - \vec{q}/2\right) \quad \text{and}$$

$$p+q = \left(\sqrt{m^2 + \vec{q}^{\,2}/4} \quad , \; + \vec{q}/2\right) \quad ,$$

where each component of p and p+q becomeslarge. Explicit calculation then shows that the behavior of $\tilde{M}_5^\mu$ for large q^2 is $(-q^2)^{-1-\delta}$, as dictated by dimensional counting[11]. Accordingly, as in the spinless calculation, we have $F(q^2) \sim (q^2)^{-1-\delta} \, \ell n(q^2/m^2)$ where the logarithm results from the endpoint of the x or y integration. The canonical renormalizable limit is $\delta \to 0^+$. As in the spinless calculation a factor $(q^2)^{-1}$ is associated with each off-shell fermion propagator, and a factor $(q^2)^{-\delta}$ with each gluon carrying large q^2 in the Born diagram. The overall scale of the form factor is determined by the value of $\psi_p^{+-}(x=0) = \int d^4k \; \psi_p^{+-}(k)$. As we have noted, $\psi^{+-}(x=0)$ is finite for $\delta > 0$.

Note that the wave function $\psi_p^{+-}(k)$ plays the same role as the spinless Bethe-Salpeter wave function. The equivalence of asymptotic behavior with spin-0 or spin-1/2 constituents follows since $\psi_p^{+-}(x)$ (see below) has the same dimensions as the spinless Bethe-Salpeter wave function, $\psi_p^{\text{spinless}}(x)$. For spinless constituents, the Bethe-Salpeter amplitude for a meson in position space is

$$\psi_p^{\text{spinless}}(x) \equiv \langle 0|T \; \phi(x)\phi(0)|p\rangle \sim [L]^{-1}$$

where we are using continuum normalization $\langle p'|p\rangle = 2\,E\,\delta^3(\underset{\sim}{p}-\underset{\sim}{p}')$ and $\langle 0|0\rangle = 1$. For the spinor case

$$\psi_p^{\text{spinor}}(x) = \langle 0|T \quad \psi(x)\psi(0)|p\rangle \sim [L]^{-2}$$

since the fermion field-operator $\psi(x)$ has dimensions $L^{-3/2}$. However, $\psi_p^{+-}(x) \sim [L]^{-1}$ since the explicit spin dependence of ψ_p is removed; accordingly the short distance behavior of $\psi_p^{+-}(x)$ and $\psi_p^{scalar}(x)$ is the same. In the language of operator product expansions at short distance the point is this: The amplitude for the large q^2 form factor of a meson composed of two quarks will involve an operator product such as $\psi_{\lambda_1}(x_1)\psi_{\sigma_1}(y_1)J_\mu(z)\psi_{\lambda_2}(x_2)\psi_{\sigma_2}(y_2)$ in a limit such as $z \approx x_2 \approx y_2$. A significant difference from say, the operator product expansion of two currents $J_\mu(x)J_\nu(0) \approx \bar{\psi}(x)\gamma_\mu\psi(x)\bar{\psi}(0)\gamma_\nu\psi(0)$ as $x \to 0$ is that in the latter case the spin of the fields is summed leaving objects (currents) whose entire angular momentum content is contained in the indices μ and ν. Therefore the operator product expansion can be made in terms of Lorentz tensors such as $\theta_{\mu\nu}$. The former case is more subtle: spinors are required to carry the spin content of the product of fields. This means that the number of degrees of freedom which determine the scaling behavior at short distances is the same as in the spin zero case.

Multiparticle bound states can be treated by a generalization of the Bethe-Salpeter techniques for two particles. For instance, the proton wave function satisfies the relation shown in Fig. 8. This time the necessary kernel for the equation is three-particle irreducible. Each aspect of the three-particle bound state analysis parallels the two-body analysis. The most important part of the spin structure of the wave function is that which reduces to a product of free quark spinors:

$$\psi_p(k_1,k_2) = u_a(k_1)u_b(k_2)u_c(p-k_1-k_2)\psi_p^{+++}(k_1,k_2) \quad . \tag{20}$$

Projecting spins correctly, there are two contributions to the wave function: 1) when a and b are in an s-state and 2) when b and c are in an s-state. The left-over quark has the helicity of the hadron.

II.A3 Short Distance Behavior of the Bethe-Salpeter Wave Function

The essential role of the finiteness condition on $\psi(x = 0)$ for the derivation of the dimensional counting rules is clear. The condition allows us to compute the high momentum transfer limit of exclusive amplitudes by iterating the kernel once and computing a minimal connected graph; thus accounting for the effects of large momentum transfer being routed through the wavefunction. Further, the values of the $\psi(x = 0)$ (which have dimensions $[\text{mass}]^{n-1}$ for n constituent fields) determine the normalization of the hadronic amplitude. In this section we will address the important question of whether the wavefunction condition is actually true in renormalizable field theories. In fact, a definitive answer has not yet been given and may well depend upon the theory. To see what is involved, consider the full Bethe-Salpeter equation, e.g., for a pion in quark-vector gluon theory (Eq. (12) and Fig. 4).

$$(\not{k} - m)(\not{p} - \not{k} - m_b)\psi_p(k) = \int \frac{i d^4\ell}{(2\pi)^4} K(k,\ell,p)\psi_p(\ell)$$

where K is the two-particle irreducible kernel. In ladder approximation to a theory with gluon mass M,

$$K_{Ladder} = \frac{g^2 \gamma_\mu^{(a)} \gamma^\mu_{(b)}}{(k-\ell)^2 - M^2 + i\varepsilon} .$$

If we suppose that K_{Ladder} gives the correct asymptotic limit, then the Bethe-Salpeter equation is singular and the power falloff of ψ depends on the coupling constant.

However, in the weak binding ($g^2 \to 0$) case, when all components of the relative momentum η become large, $\psi \sim \eta^{-4}$ modulo log η. This result was first obtained by Salpeter[10] for the instantaneous (coulomb) ladder approximation.

Serious objections can be raised to the use of the ladder approximation in the strong binding theory for determining the true asymptotic behavior of the Bethe-Salpeter wavefunctions:

(1) The ladder approximation result for the asymptotic limit is unstable under the perturbation of adding additional kernels (e.g., the crossed-graphs, vacuum polarization, vertex corrections, etc.). In each case the power dependence on the relative momentum is changed.

(2) The behavior of ψ at large relative momentum determined from ladder approximation is discontinuous as the dimensional regularization (4-d) for loop integrations is taken to zero. If it is argued that the physical solution for quantities such as the asymptotic behavior of $F(q^2)$ must be analytic as a function of 4-d, then the wave function at the origin is finite.

(3) The ladder approximation can only be valid in a limited range of coupling constants. When g^2 becomes too large, the energy eigenvalue becomes imaginary, indicating a non-hermiticity of the equation. One can see this explicitly from the Salpeter equation. The situation is analogous to the familiar situation for the strong binding limit of the Dirac-Coulomb equation with $V = - Z\alpha/r$. For the lowest eigenstate, we have

$$\varepsilon_{1s} = \sqrt{1 - (Z\alpha)^2}\; M$$

$$\psi_{1s}(r) \sim r^{-1+\sqrt{1-(Z\alpha)^2}} \qquad (\text{for } r \sim 0) \quad .$$

The singular equation has no physical solution for $Z\alpha > 1$: it is undefined. Regularization of the potential for $r \sim 0$ is thus required. The standard procedure is to make V less singular than r^{-1} for a region around $r \sim 0$ (which of course occurs physically due to the finite mass of the source). Then ε_{1s} is real and $\psi_{1s}(r = 0)$ is finite for all $Z\alpha$[12]. For very large $Z\alpha$ a multiparticle pair creation is required.

There is reason to believe that in renormalizable theories the full kernel K is, in fact, more convergent asymptotically than K_L. As we conjectured in Ref. 1, asymptotically free theories are likely to give rise to a wavefunction whose singularity at $x = 0$ is at most a power of a logarithm. This is heuristically plausible since as the characteristic momenta in a graph become larger and larger relative to masses, the effective coupling constants become smaller and smaller, so that the weak binding result holds. If it is legitimate to imagine taking the limit $q^2 \to \infty$ before summing the perturbation series then the wavefunction condition holds, modulo a power of a logarithm. Recently Appelquist and Poggio[13] have shown that in a ϕ^3 theory in six dimensions, which is asymptotically free, the renormalization group can be used to demonstrate that the wavefunction is finite at the origin up to a calculable logarithm. However, they emphasize that the infrared corrections to the interactions among constituents may lead to further logarithmic corrections. (See Sec. II.B3 for our discussion of this point.)

Even in renormalizable theories which are not asymptotically free, the vertex and vacuum polarization corrections to the gluon exchange diagrams in the complete kernel may well damp the asymptotic behavior of K, as do the finite size corrections to the Coulomb potential. Thus there are both physical and mathematical reasons to believe that the full kernel is sufficently regular that the wavefunction at short distance is finite or at worst logarithmically singular. Clearly this problem deserves further study.

Suppose that the wavefunction is not finite at $x = 0$. There are two possibilities: it diverges or is zero. If the wavefunction diverges with a power δ it modifies the effective n_h associated with that hadron, so, e.g., for a meson $n = 2 - \delta$ rather than 2. Similarly if it diverges or vanishes logarithmically it induces logarithmic deviations from perfect scaling.

If the wavefunction vanishes as a power at $x = 0$, the next-to-leading Born terms will determine the asymptotic behavior of the matrix element. This is the case when a bound state has non-zero orbital angular momentum[14], at least if the wavefunction's dependence on energy and three-momentum factorizes in the hadron rest frame. That is, if $\psi_P(q)$ can be written as $\psi_P(q_0)\phi(\underset{\sim}{q})$, then $\phi(\underset{\sim}{r}) \sim r^L$ times angular factors. Hence for a two-constituent bound state of orbital angular momentum L, $\psi(x \sim 0) \sim x^L \sim m^{-L}$ when all components of x are proportional to each other and small. The result is to cause further damping of matrix elements. Hence the form factor of an $L = 1$ state should have the asymptotic behavior $(q^2)^{1-n-L}$. Effects of orbital angular momentum have been considered in more detail by Amati et al.[36] and Ciafaloni[15].

In addition to the finiteness of the wavefunction at the origin in coordinate space, assumption A included the requirement that it is bounded at every point in momentum space. Although this latter condition is difficult to prove directly by studying the Bethe-Salpeter equation[13], there can be little doubt about its validity as long as quarks are not observed experimentally (because if the wavefunction is bounded everywhere in coordinate space but of finite "volume" then its Fourier transform is necessarily finite).

II.B Irreducible Diagrams

An important conclusion of Section II.A is that, given sufficient short distance smoothness of the wavefunction (assumption A), the irreducible amplitudes (the M_n) determine the high energy, fixed angle behavior of the full amplitude. This section is devoted to discussing the conditions under which the irreducible amplitudes obey naive dimensional scaling, i.e. $M_n \sim \sqrt{s}^{\,4-n}$ asymptotically.

II.B.1. Landshoff Diagrams

As mentioned in the introduction to this section, Landshoff[7] has recently emphasized a class of diagrams which, if present, would violate dimensional scaling. Such a diagram is shown in Fig. 9. It is characterized by having fewer off-shell fermions than standard diagrams for the same process such as shown in Fig. 10. In fact, for meson-meson and baryon-baryon scattering no fermion line need be far off shell. Physically, it corresponds to (say for meson-meson scattering) the independent, elastic, on-shell scattering of pairs of constituents such that the final momenta are properly aligned. Landshoff calculated their asymptotic behavior and found, using a Sudakov parameterization, that for meson-meson scattering $M \sim s^{-3/2} f(t/s)$ and for baryon-baryon scattering $M \sim s^{-3} f(t/s)$, in contrast to the dimensional result $M \sim s^{-2}$ and s^{-4} respectively. We have verified his results using both Feynman parameterization[16] and infinite momentum frame perturbation theory (see Appendix A). The kinematic configuration (see Fig. 11) which gives the pinch has all the quarks near mass shell so the two elementary quark-quark scatterings at large momentum transfer are dimensionless since n = 4. The energy dependence of the full amplitude arises from the condition that the final momenta be aligned properly. Referring to Fig. 11 we can see how $s^{-3/2}$ comes about; the center of mass frame of the two mesons is convenient for this purpose. For definiteness, label the momenta of the quarks so

x_1 and x_2 are less than 1/2. Examining Fig. 11b, it is evident that in order for the final quarks to have nearly parallel momenta (so the transverse momenta of the quarks in the final mesons are finite as required by the wavefunction) it is necessary that $x_1 = x_2 + O(\frac{1}{P})$ where P is the magnitude of the meson 3-momenta in the center of mass ($P \sim \sqrt{s}$). Assuming then that $x_1 \approx x_2$ we have the configuration shown in Fig. 11b. Imagine that the quarks with fraction $x_1 \approx x_2$ scatter by some finite angle θ. Momentum conservation means that $x_1 = x_2 = y_1 = y_2$ within $O(\frac{1}{P})$. Let their plane of scattering define the x - z plane. Now consider the scattering of the quarks with fractions $(1-x_1) = (1-x_2) + O(\frac{1}{P})$. They in general scatter in some different direction having polar angle θ' and azimuthal (relative to the xz plane) angle ϕ. Since they carry a very large 3-momentum $(1-x_1)P$, they will carry large momentum transverse to the direction defined by the other set of quarks unless $\phi' = \phi + O(\frac{1}{P})$. Thus there are three constraints on the kinematics, each requiring a parameter normally allowed some finite range to be restricted to a range $O(\frac{1}{\sqrt{s}})$. Hence $M \sim s^{-3/2}$ and $\frac{d\sigma}{dt} \sim s^{-5}$ (rather than s^{-6} as given by Eq. (1)).

Technically, the near-mass-shell diagrams have a stronger asymptotic behavior than the scaling law because of pinch singularities that arise in the integrals over the constituent momenta. This gives rise to an anomalous dependence on the quark mass not present in diagrams whose leading behavior results from an end point singularity in the Feynman integral. That is, a linear infrared divergence in the quark mass serves to define a fundamental length scale: $\frac{1}{m_q}$. To illustrate how this occurs in practice, we give in the Appendix A an infinite momentum frame calculation of the Landshoff contribution to meson-meson scattering. As can be deduced from the above analysis, there will be no modification of naive scaling by such a mechanism for lepton-hadron scattering, Compton scattering or photoproduction[17].

This class of near-mass-shell scattering diagrams should evidently dominate the hadron scattering amplitudes in the asymptotic limit[18]. Their existence implies a violation of Eq. (1) for meson-baryon and baryon-baryon scattering, giving instead

$$\frac{d\sigma}{dt} \sim \frac{s^{L-1}}{s^{n-2}} \; f(t/s) \quad , \tag{21}$$

where L is the number of wide angle, on-shell quark scattering, e.g., L = 2 for meson-baryon scattering and L = 3 for baryon-baryon scattering. Experiment (see Section III and Ref. 18) favors the dimensional scaling result of Eq. (1). From this we learn a striking fact about nature which is incorporated in assumption C; multiple near-mass-shell scattering is <u>not</u> important for present experiments.

The validity of assumption C is much more difficult to understand theoretically than the validity of A and B although their ultimate explanations may well be connected. Polkinghorne[19] has recently advocated adoption of a somewhat stronger version of C: that large angle scattering of near-mass-shell quarks is damped in energy. A possible mechanism for this damping is an accumulation of logarithms in the corrections to the quark-quark-gluon vertex when both quarks are near mass shell[20].

Another proposal, made earlier and for a different purpose by Blankenbecler, Brodsky and Gunion[21], is that gluons cannot be exchanged between quarks of different hadrons, or else that the amplitude for gluon exchange is very small. Their analysis indicates that the constituent-interchange picture gives a good description of the angular dependence of exclusive scattering with no gluon exchange required (in this connection see our discussion of asymptotic Regge trajectories, Sec. II.B3). Since a field theory with quarks and gluons would in general have both quark interchange and gluon exchange, this indicates that gluon exchange is suppressed in nature. Further evidence for this proposal is given in Sections

II.B3 and IV. It should be emphasized however, that this is essentially a phenomenological rule: a consistent description of present wide angle experiments can be made with no gluon exchange whatever. No compelling theoretical reason for this rule has yet been advanced.

Yet another possibility is that in a model with permanently confined quarks such near-mass-shell processes would be suppressed. It can be heuristically argued that, since this contribution is proportional to $\frac{1}{m_q}$, if the effective quark mass were very large (perhaps comparable to $\sqrt{s}$) it would be small. From the time-ordered perturbation theory calculation of the Appendix it can be seen that the internal state with near-mass-shell quarks (which in a color SU(3) theory[22] has non-zero color systems propagating) exists for a finite time, long compared to $s^{-1/2}$. Such a state might be suppressed in the full amplitude.

II.B2 The Irreducible Diagrams

Typical Born diagrams for meson-baryon scattering and meson photoproduction are shown in Figs. 10 and 12. The heavy dots indicate which fermion propagators are far off mass shell. With scalar constituents having ϕ^4 coupling, the wavy lines just reduce to a point interaction. By applying the mnemonic of Section II.A1 and II.A2 (s^{-1} for each off-shell fermion) the diagrams of Fig. 10 are immediately seen to have the asymptotic behavior $M \sim (\sqrt{s})^{4-n}\ f(t/s)$ in the limit $\delta \to 0^+$. Hence they reproduce Eq. (1). The only process which needs special discussion is photoproduction (Fig. 12).

According to dimensional counting, if the photon counts as one field the photoproduction amplitude should $\sim (\sqrt{s})^{4-n}$. Fig. 12 shows that three fermion propagators are large (as in the meson-baryon case of Fig. 10). However (as the reader can easily verify by direct calculation) the vector coupling of the photon introduces a numerator factor proportional to $\sqrt{s}$ resulting in the expected behavior $M_9 \sim s^{-5/2}$. This is characteristic of the vector coupling, not the spin of the constituent and occurs for either spin-0 or -1/2 quarks. Had the quark anti-quark pair (looking in the photon channel) been constrained to have limited relative momenta, which a hadronic wave function would do, the photon coupling would not have generated a $\sqrt{s}$ so that $M \sim s^{-3}$. This is the vector meson dominance contribution to photoproduction at large s and t.

Fig. 13 shows typical Born diagrams for the proton form factor with spin 1/2 constituents. It is readily seen that for either scalar or vector gluon exchange (helicity flip or non-flip respectively in the zero-quark-mass limit) graphs of the kind shown in Fig. 13b give a leading contribution $\sim (q^2)^{-2}$ to $F_1(q^2)$. When $q^2 \gg m_q^2$ the diagram of Fig. 13a cannot contribute for scalar gluons. Explicit calculation shows that $F_2(q^2)$ is proportional to m_q^2 so that in general a three-quark model of the proton form factor will give $F_2(q^2) \sim F_1(q^2)/q^2$ when q^2 becomes large. In terms of the commonly used form factors $G_E(q^2) \equiv F_1(q^2) + \frac{\kappa q^2}{4M^2} F_2(q^2)$

and $G_M(q^2) \equiv F_1(q^2) + \kappa F_2(q^2)$ where κ is the anomalous magnetic moment, this corresponds to[23] constant G_E/G_M at large q^2 as is indicated experimentally (Section III).

We noted above that meson-baryon scattering or indeed any hadronic scattering, could take place either by gluon exchange between the hadrons or by quark interchange (Fig. 10b and 10c). Both give the same scaling behavior but in general they give rise to very different angular distributions (i.e., the function $f(t/s)$ which we leave unspecified depends on the relative importance of the two types of diagrams). Although we do not attempt here to deal with the problem of the complete angular distributions, we are able to make some statements about the kinematic region to very large, $s \to \infty$. When t and s are both large we know the overall power dependence of $d\sigma/dt \sim s^{-n+2}\, f(t/s)$ but not in general the function $f(t/s)$. However, if either gluon exchange or quark interchange is the dominant t channel process (see Fig. 14) we can specify the form of $f(t/s)$.

Using Regge terminology we write the amplitude as $M \sim s^{-\alpha_{eff}(t)}\, \beta(t)$. As is well known, a spin 1 or spin 0 gluon in the t channel gives rise to a constant $\alpha_{eff}(t) = 1$ or 0 respectively for all t. Multigluon exchanges only generate cut corrections. When quarks are interchanged there are two important regions in the integration over the intermediate quark momenta: $k \sim xP_C$ or $k \sim xP_A$. Consider the former. In this case the lower half of the diagram is purely a function of $t = q^2$ (just as in a form factor calculation). In fact it has the same asymptotic t dependence as the helicity non-flip form factor $F(t) \sim t^{-n_C+1}$. The upper part of the diagram when $s \gg t$ is also simple. It is essentially high energy, $\text{quark}_1 + A \to \text{quark}_2 + B$ scattering. An explicit t dependence comes from that required by helicity considerations[24]: $\sqrt{t}^{\,|\lambda_1+\lambda_A-\lambda_B-\lambda_2|}$. Hence for A = B = meson or A = B = baryon the leading behavior is t independent. On the other hand, for π photoproduction the upper blob $\sim \sqrt{t}$. Thus we find that for meson-baryon scattering $M \sim s^{-3} f(t/s) \sim s^{-\alpha} F(t)$; there are two terms (coming from

$k \sim xP_C$ and $k \sim xP_A$) proportional to $F_p(t)$ and $F_\pi(t)$ respectively. The leading behavior in s comes from F_p so we have with quark interchange $\alpha_{eff}^{MB\to MB} = -1$. Similarly $\alpha_{eff}^{BB\to BB} = -2$ and $\alpha_{eff}^{\gamma B\to MB} = -1$[25].

According to Ref. 26 the best fits to α_{eff} are indicative that gluon exchange is negligible. Since a priori counting coupling constants (e.g., in Fig. 10) indicates that gluon exchange and quark interchange should be equally important, this gives support to the proposal of the previous section that gluon exchange between quarks of different hadrons is anomalously small. Hence it provides additional support to our assumption C.

II.B3 Higher Order Corrections to the Born Diagrams

In any given order of perturbation theory there will be logarithmic corrections to the behavior of the Born diagrams due to loop integrals. If these logarithms were to coherently combine they could conceivably alter the simple scaling behavior of the Born amplitude. For instance, in QED it has been shown[27] that infrared radiative corrections to fixed angle exclusive lepton and photon scattering amplitudes have the form

$$e^{-\alpha[\ln(s/\lambda^2)]^2} \quad , \tag{22}$$

where t is the momentum transfer and λ an effective infrared cutoff.

We are concerned with the possible exponentiation of logarithms due to strong interaction corrections to a bound state scattering amplitude. In a gauge theory it is the infrared region which is potentially dangerous in this respect. It is possible that they will introduce a modification to these amplitudes of the form of Eq. (22). In that case the scattering rules (Eqs. (1-4)) will just give the nominal or canonical power law reflecting the compositeness of the hadron, but which will be modified by soft interactions among the constituents. If the fundamental strong interaction coupling is actually weak, as conjectured by a number of people[28], such a modification would not be seen until very large t.

On the other hand, arguments can be made that the infrared effects on a bound state scattering amplitude should be much milder than Eq. (22) for two reasons: First, in a theory such as a color non-abelian gauge theory[22] the physical states are neutral, i.e., color singlets, so that the infrared region is damped for momenta $k < O(d^{-1})$ where d is a length characteristic of the hadron. Second, in a bound state the constituents are generally off their mass shells and hence the infrared singularities are "shielded."

To illustrate the first point, consider an abelian gauge theory in which massless vector mesons couple to a conserved current. We shall take a hadron to be a neutral state, so that $Q = \sum_i Q_i = 0$. Using Weinberg's[29] notation, the infrared region of the virtual gluon corrections ($\lambda < |k_\mu| < \Lambda$) gives a correction factor to the scattering matrix element of the form $\exp[-A \ln \Lambda/\lambda]$ with

$$A = \frac{-1}{8\pi^2} \sum_{mn} \eta_n \eta_m Q_n Q_m \beta_{nm}^{-1} \ln\left[\frac{1+\beta_{nm}}{1-\beta_{nm}}\right], \tag{23}$$

where the summation is over all pairs (n,m) of external charged lines. For an outgoing (incoming) line $\eta = +1$ (-1) and β_{nm} is the relative velocity of particles n and m in the rest frame of either:

$$\beta_{nm} = \left[1 - \frac{P_n^2 P_m^2}{(P_n \cdot P_m)^2}\right]^{1/2} . \tag{24}$$

Considering now an amplitude such as the form factor of a "meson," we must sum Eq. (23) over all pairs of external lines. It is readily checked that the only terms in the sum (23) which can introduce a leading t dependence are those involving one initial and one final particle. Let us label the two (say) initial particles a and b whose momenta are $p_a = xp + \kappa$ and $p_b = (1-x)p - \kappa$ with $\kappa \cdot p = 0$ (as in Section II,A1). By our assumption A, κ is bounded so that (as may be checked by explicit expansion of the logarithm in Eq. (23)) we may take $p_a = xp$ and $p_b = (1-x)p$ with errors of only order 1/s at fixed angle. Then β_{an} and β_{bn} are equal if n is not equal to a or b. Summing over a and b in Eq. (23) thus causes cancellation of the infrared corrections of order $\ln(t/m^2)$ since $Q_A = - Q_B$.

The infrared behavior of non-abelian theories with massless vector gluons is generally expected to be much worse than in the abelian case. A central difficulty of such theories is that a soft gluon emitted from an external line can itself emit a pair of soft, colored massless gluons, ad infinitum. However, in a bound state such catastrophic gluon emission may well be regulated by virtue of the gluon constituents of the hadrons being effectively off-mass-shell.

Furthermore, in the case of a color theory as usually envisioned[22], color octet hadrons either are infinitely massive or at least not degenerate in mass with the usual hadrons which are color singlets. In this case the infrared contribution for k^2 and $p \cdot k$ below $m_8^2 - m_1^2$ is suppressed, giving corrections of order $\log [t/(m_8^2-m_1^2)]$. Moreover because the color emission changes quantum numbers and is not soft, there is no reason that such logarithms will exponentiate or cause large corrections to the scaling law[30].

Even if the logarithms found in perturbation theory do not exponentiate, as argued above, they can give logarithmic corrections to the scaling laws. There is very little we can say about this (essentially about the validity of assumption B) except what we said in Ref. 1: if there are modifications of scaling in deep inelastic scattering, there will probably be similar modifications to these scaling laws[31].

III. The Experimental Status of Exclusive Scaling

In this section we are concerned with tests of the scaling law (Eq.(1)) in exclusive processes. Three questions are of particular importance: 1) Is our choice of quark model assignments for the number of fields in hadrons acceptable? 2) Are the scaling laws actually exact or are they perhaps modified by logarithmic or "anomalous dimension" corrections? 3) Are there contributions from on-shell scattering (which may change the scaling of Eq.(1))? Of course, essential to the whole program is the self-consistency of the scheme. Once that is established for exclusive processes, we turn to the more difficult question of inclusive scattering. This section is quite detailed, in the hope of emphasizing (especially to experimentalists) the large amount of important work which needs to be done in this field.

The simplest applications of Eq. (1) are purely electrodynamic, e.g., $e^+e^- \to \mu^+\mu^-$ or $e^+e^- \to e^+e^-$, $\gamma e \to \gamma e$, $e^+e^- \to \gamma\gamma$, etc. In each of these cases n = 4 unless we are wrong at a fundamental level, so that experimentally these should have the asymptotic behavior $d\sigma/dt \sim s^{-2} f(t/s)$. This is just the prediction of quantum electrodynamics (modulo logarithms from radiative corrections) so that to the extent that QED is correct at large s and t our predictions for the scaling behavior of purely leptonic and photonic processes are correct with the assignment n = 1 for leptons and photons. Since QED is in agreement with experiment up to the highest available s and t (CEA[32] and SPEAR[33] results on $e^+e^- \to \mu^+\mu^-$, $e^+e^- \to e^+e^-$, etc.) we may assume that n = 1 is correct for leptons.

In one-photon exchange approximation, the differential cross section for eh → eh scattering at very large s and large t is given in terms of the hadron spin averaged electromagnetic form factor F(t) by

$$\frac{d}{dt} \sim \frac{1}{t^2}|F(t)|^2 \tag{25}$$

so that we have (Eq. (2)) the general formula (modulo logarithms)

$$F_h(t) \sim t^{1-n_h} \quad ,$$

for asymptotic spacelike or timelike t. Thus using $n_\pi = 2$ and $n_p = 3$, we conclude that for large q^2, $F_\pi(q^2) \sim (q^2)^{-1}$ and $F_{1p}(q^2) \sim (q^2)^{-2}$ can be separately determined by studying the dependence of $ep \to ep$ scattering on q^2. As remarked in Section II.B2, given spin 1/2 constituents with vector or scalar gluon exchange, one finds that $F_2(q^2) \sim (q^2)^{-3}$ at large q^2, so that we predict the asymptotic behavior $G_E \sim 1/q^4$ and $G_M \sim 1/q^4$ [23]. Since a substantial range of large q^2 is necessary to test these laws, the experiment of P. N. Kirk et al.[34] covering the spacelike range $1.0 \leq -q^2 \leq 25.0$ GeV^2, is most suitable for our purposes. Fig. 15 shows $q^4 G_M(q^2)$ for that experiment. For $-q^2 > 4$ GeV^2, $q^4 G_M(q^2)$ is consistent with a constant within errors. This vindicates our choice $n_p = 3$ as suggested by the naive quark model. Moreover the very fact that $G_M(q^2)$ falls as a power of q^2 is support for our scaling laws. (The data is not accurate enough to discuss the question of logarithms.) G_E and G_M have been separately determined only for $-q^2 \lesssim 3.75$ GeV^2.[35] They are found to be consistent with $G_E = G_M/\mu$ within errors. The asymptotic falloff of the proton form factor has proved very difficult to account for up to now. Bound state models for simplicity have focused on two-particle bound states. Treating the proton as a spin-0, spin-1/2 bound state with spin-0 exchange gives[36] (modulo logs) $G_M \sim (q^2)^{-2}$ but $G_E \sim (q^2)^{-1}$. Separate determination of G_E and G_M at larger q^2 will be useful to conclusively distinguish this model from ours. However, it is improbable that G_E could have the behavior $(q^2)^{-1}$ without that being evident from the q^2 dependence of the $ep \to ep$ cross section[37].

Data on the pion form factor is not yet available for a q^2 range comparable to that of the proton since it comes from e^+e^--annihilation. Presently data is available[38] for timelike $q^2 < 9.0$ GeV^2. It is consistent with a ρ pole, so that for q^2 large, $F_\pi(q^2) \sim (q^2)^{-1}$ is an acceptable fit (see Fig. 16). However, it should be kept in mind that to conclusively test our picture, $q^2 \gtrsim 4\ \mathrm{GeV}^2$ should be considered. If only that range is used, the data is not adequate to rule out other behavior. Improving and extending measurements of the pion form factor is one of the surest ways to verify or destroy our ideas. For the present we will continue to assume $n_\pi = 2$. In a ladder model in which the pion is a bound state of two spin-0 constituents with ϕ^3 interactions its form factor would fall as $(q^2)^{-2}$.

According to the dimensional scaling rules, if a photon behaves as a single field at short distances, photoproduction at large s and t follows $\frac{d\sigma}{dt} \sim s^{-7} f(t/s)$. This is an especially interesting process because strict vector meson dominance would say that $\gamma p \to \pi p$ behaves like $\rho p \to \pi p$ and hence $\frac{d\sigma}{dt} \sim s^{-8} f(t/s)$. Of course if the photon, when interacting with hadrons, is a superposition of a vector meson and an elementary field[39], then in the kinematic region being studied here the latter state will dominate and result in $d\sigma/dt \sim s^{-7} f(t/s)$. The highest energy data at 90° is that of R. L. Anderson et al.[40] which covers the range E_γ between 4 and 7.5 GeV. They find that $d\sigma/dt\ (90°) \sim s^{-7.3 \pm 0.4}$, in agreement with our prediction of s^{-7}. Again, it is most desirable to extend the range of s, since at $E_\gamma = 4$ GeV, 90° corresponds to a t of about 3 GeV^2 which we expect is only barely in the scaling region. However, if that lowest energy point is dropped, little can be said about the s dependence of $d\sigma/dt$ at 90°. Thus our provisional conclusion is that photoproduction measurements support the prediction that $d\sigma/dt\ (\gamma N \to \pi N) \sim s^{-7} f(t/s)$, with higher energy data of great importance.

The present data on meson-baryon scattering, which we expect to behave as $d\sigma/dt \sim s^{-8} f(t/s)$ at large s and t, is less conclusive for our purposes than photoproduction or pp scattering experiments. This is partly because experiments to date have focused on obtaining the entire angular distribution at modest s values rather than choosing some small θ_{cm} range with enough sensitivity to go to high values of s. This poses the usual problem of not having an adequate range of high enough s and t to check for scaling. A special problem in some of these meson-baryon scatterings is the existence of (resonance?) structure at quite high t values. For instance in $\pi^- p \to \pi^- p$ a dip in $d\sigma/dt$ is found at $t = -3.8\,(\mathrm{GeV}/c)^2$ [41] and there is evidence that both $\pi^{\pm}p$ have a dip at $t = -4.8\,(\mathrm{GeV}/c)^2$. For an unambiguous analysis, one needs for this process t and $u \gtrsim 5\,(\mathrm{GeV}/c)^2$ and a large range of s! One experiment which has been analyzed to determine the nature of the wide angle energy dependence measures the 90° differential cross sections for $\bar{K}^0 p \to \pi^+ \Lambda^0$, $\bar{K}^0 \to \pi^+ \Sigma^0$ and $K_L^0 p \to K_S^0 p$ for incident momenta between 1.0 and 7.5 GeV/c[42]. They find that their results can be equally well parameterized by $(d\sigma/d\Omega)_{90°} \sim s^{-m}$ or $(d\sigma/d\Omega)_{90°} \sim s^{-bp}$ (see Fig. 17). If s and t are sufficiently large, $d\sigma/d\Omega \sim s\, d\sigma/dt\, f(t/s)$ so that we predict $m = 7$. They give for the three reactions $m = 7.4 \pm 1.4$, $m = 8.1 \pm 1.4$, and $m = 8.5 \pm 1.2$ respectively. In short, our predictions are consistent with data on meson-baryon scattering, but it only demonstrates that we are not wildly wrong. However, results from experiments which only attempt to cover the large angle region, but with much higher sensitivity (so that a larger range of s can be studied) will be much more conclusive. It is enough to show that the cross section integrated over a fixed cm region falls with the power s^{-7} rather than another power or an exponential.

Not surprisingly, $pp \to pp$ is the most thoroughly studied elastic process at large s and t. Landshoff and Polkinghorne[8] have plotted the data for $s > 15\ \mathrm{GeV}^2$ and θ_{cm} between 38° and 90° (see Fig. 18). They find that it is well fit by the form $d\sigma/dt \sim s^{-9.7 \pm 0.5} f(\theta)$. This is in very good agreement with our prediction $d\sigma/dt \sim s^{-10} f(\theta)$, and [43] apparently rules out a significant contribution to the amplitude by on-shell quark scattering[18].

The experimental evidence on Eq. (1) is thus very encouraging. However with little difficulty it could be considerably improved. As indicated above, better data on meson-baryon scattering and $e^+e^- \to \pi^+\pi^-$ should be available fairly soon and will be a significant test of the scaling idea. We close this section with a list of predictions of the scaling law of Eq. (1); other reactions whose asymptotic behavior is interesting, albeit difficult to measure:

$$\gamma p \to \gamma p \qquad d\sigma/dt \sim s^{-6} f(t/s)$$

$$\gamma p \to \rho p \qquad d\sigma/dt \sim s^{-7} f(t/s)$$

$$\gamma\gamma \to \pi\pi \qquad d\sigma/dt \sim s^{-4} f(t/s)$$

(the photons need not have zero mass as long as their masses are kept fixed and are small compared with s and t)

$$e\gamma \to e\pi^0 (\gamma^* \gamma \to \pi^0) \qquad d\sigma/dt \sim s^{-3} f(t/s)$$

$$e^+e^- \to A_2^+ A_2^- \qquad F_{A_2}(q^2) \sim (q^2)^{-2}$$

(or any other L = 1 meson with non-vanishing form factor)

$$ed \to ed \qquad F_d(q^2) \sim (q^2)^{-5}$$

(this probably only scales for $q^2 \gtrsim 8\text{GeV}^2$). Finally, the scaling law for multi-particle exclusive large angle scattering (Eq. (3)) can be tested. When $n_M = 2$ and $n_B = 3$ it can be written in a compact form: Let $\Delta\sigma$ be the invariant cross section integrated over some fixed cm angular region keeping all ratios $\frac{p_i \cdot p_j}{s}$ $(i \neq j)$ fixed. Then when $s \to \infty$ as the reader can easily verify (Eq. (4))

$$\Delta\sigma \sim s^{-(1+N_M+2N_B)} f\left(\frac{p_i \cdot p_j}{s}\right)$$

where N_M and N_B are, respectively, the total number of mesons and baryons. Thus for high energy $BB \to MBB$ when all cm angles are large $(E_\pi \, d\sigma/dt \, d^3p_\pi) \sim s^{-12} f(\theta_i)$ which is equivalent to $d\sigma/d\Omega_1 d\Omega_2 \sim s^{-10}$. Data expected at SPEAR and DORIS on the exclusive channels $e^+e^- \rightarrow \pi^+\pi^-\pi^+\pi^-$ and $e^+e^- \rightarrow 6$ charged π's with fixed angles will eventually provide a test of our predictions ($\Delta\sigma \sim s^{-3}$ and $\Delta\sigma \sim s^{-5}$ respectively).

IV. Inclusive Reactions at High Transverse Momentum

Having developed in previous sections the rules for determining the power dependence of exclusive scatterings at large energy and momentum transfer, we wish to explore their implications for high $p_\perp$ inclusive scattering[44]. It is to be expected that, just as in the exclusive case, the power dependence of inclusive high $p_\perp$ cross sections will depend on the number N of constituents participating in the high $p_\perp$ reaction. Our task, then, is to see what can be said about this number N.

In parton language, an exclusive process proceeds by the large momentum scattering of n constituents with the wee partons behaving as "spectators." The condition on the bound state wave function at $x = 0$ serves two purposes: First, it fixes the minimum number of constituents having finite fraction of the total momentum (and hence n). Second, it ensures that the remaining "wees" are truly "spectators," that is, their interactions do not build up additional power dependence on momentum transfer. (This latter function is modified if the wave function in nature proves to have a logarithmic or power singularity at the origin).

In inclusive scattering, constituents having finite fractions of the momenta of the incident particles can be spectators. A good example of this is deep inelastic scattering in the parton model, shown in Fig. 19a. In the absence of a requirement that no particles be found in the forward direction, it is energetically favorable for those partons not deflected by the current to continue without large changes of their transverse or longitudinal momenta. In this case only the single parton with appropriate momentum fraction $x = -q^2/2m\nu$ need participate in a large momentum transfer collision. Hence $n = 4$ (2 leptons and 2 quarks) so that the matrix element is dimensionless and the differential cross section $E_e d\sigma/d^3p_e \sim s^{-2}\ f(q^2/s, M^2/s)$ asymptotically

(M is the missing mass). In the one photon exchange approximation, this differential cross section may be written in terms of structure functions W_1 and νW_2 which are defined in such a way that they have no energy (ν) dependence for fixed (q^2/ν) if the behavior of the differential cross section is $1/s^2$ as argued above. The famous scaling behavior of νW_2 seen at SLAC, if it persists at higher energies, is evidence for the validity of this argument. A logarithmic modification of scaling as expected in asymptotically free theories is not distressing:that is just the effect in such theories of the interactions of the "spectators."

Motivated by the success of the scaling prediction in deep inelastic scattering, we abstract the notion that any inclusive amplitude factorizes into a part which involves only large momentum transfers and parts involving only low momentum transfers. That part depending on the large momentum transfers determines the overall power dependence of the amplitude. Of course the dependence of the cross section on invariant ratios, say $\frac{t}{s}$ and $\frac{M^2}{s}$, is in general dependent on the low as well as high momentum parts of the scattering process. Thus we can immediately write down (Eq. (5)) the invariant cross section for high energy inclusive scattering at fixed t/s and M^2/s:

$$\frac{E\, d\sigma}{d^3p} \sim \frac{1}{s^{N-2}}\, f\left(\frac{t}{s},\frac{M^2}{s}\right)$$

with N defined as the minimum of fields in the large momentum transfer part of the amplitude.

Evidently, in order to make predictions for inclusive scattering, one must make a dynamical statement which serves to specify the number of fields N, just as in the exclusive case a specification of the number of non-wee constituents was required. The simplest ansatz for N is the one made by Berman, Bjorken and Kogut[45] in what was essentially the first parton model work on high transverse momentum inclusive processes. They observed that at order α^2 hard parton-parton scattering must take place via exchange of a far off-shell photon just as lepton-parton scattering does in deep inelastic scattering (Fig. 19). Presumably, hadronic final states would be generated from the quarks just as in the lepton scattering case, i.e., in a scale invariant manner. If the large momentum transfer process is $qq \rightarrow qq$ or $q\bar{q} \rightarrow q\bar{q}$, N = 4, and in fact Berman, Bjorken, and Kogut predicted

$$E \frac{d\sigma}{d^3p} \sim \frac{\alpha^2}{s^2} f(\frac{t}{s}, \frac{M^2}{s}) .$$

However, it was natural to imagine that such a $qq \rightarrow qq$ scattering at high $p_\perp$ could take place via the exchange of vector (or scalar) gluons as well as via a photon. In fact in perturbation theory it is hard to imagine that gluons could be responsible for binding of quarks and yet not give rise to wide angle quark scattering, leading to the scaling behavior $E\, d\sigma/d^3p \sim s^{-2}$ at a level well above that due to electromagnetism.

In an alternative approach, Blankenbecler, Brodsky, and Gunion[46] explored a model in which hadrons scatter not by gluon exchange but by quark "interchange." They argue that the resulting angular distributions for wide angle elastic scattering are in good agreement with data, with no gluon exchange necessary for their fit (see Section II.C). In their model, hard parton-parton scattering which takes place via gluon exchange is not allowed. The minimal large $p_\perp$ processes which can take place in this case involve quark-hadron scattering and thus $N \geq 6$. In addition it makes quite detailed predictions on the function $f(\frac{t}{s}, \frac{M^2}{s})$ of Eq. (5). Thus the details of the model will be subject to many experimental checks.

Here rather than advocate any particular model we categorize and discuss the possibilities. Our principle contribution to this subject is merely the observation that the essential element of any model of high $p_\perp$ inclusive scattering, as far as the overall power of s goes, is the number of large $p_\perp$ participants. If the minimal large $p_\perp$ reaction is $qq \to qq$ or $q\bar{q} \to q\bar{q}$ then $N = 4$ as discussed above. If for some reason that is not possible or is dominated by other processes giving a large $p_\perp$ meson, such as $q\pi \to q\pi$, $qq \to \pi qq$ or $q\bar{q} \to \pi\pi$, then $N=6$ or more. If the process of interest is, say $\gamma p \to \pi + X$ then the high $p_\perp$ reaction might be $q + \gamma \to \pi + q$ or $\bar{q} + \gamma \to \pi + \bar{q}$ giving $N = 5$.

For baryons observed in the final state, say $pp \to p + X$ or $\pi p \to p + X$, there are several possible $N > 4$ reactions: $qq \to p\bar{q}(N=6)$, $qp \to qp(N=8)$, $q\bar{q} \to p\bar{p}(N=8)$, etc. The lack of an $N = 6$ process with a $\bar{p}$ produced involving only quarks in the initial state would predict that the cross section for $pp \to \bar{p} + X$ should be much smaller than in $pp \to p + X$ at large $p_\perp$, away from the edge of phase space. This is only a sample of the rich phenomenology available when looking at inclusive processes from this point of view.

The experimental results on large momentum transfer scattering[47] have one remarkable feature in common. They are not consistent with the power dependence $E\, d\sigma/d^3p \sim s^{-2}$ at fixed $p/\sqrt{s}$ and $\theta = 90°$, i.e., $p_\perp^{-4}$. Rather they favor much more rapid falloff in $p_\perp$ with a power between -8 and -11. The details of how their results are described in terms of the phenomenology outlined above is given in the references of 44. What is of greatest importance here is that the absence of $p_\perp^{-4}$ behavior is strong phenomenological support for the absence of scale invariant scattering between quarks of different hadrons and hence for our assumption C.

Equation (5) suggests a new way of analyzing the data on deep inelastic scattering. The standard method is to take the observed experimental cross section, assume that the one-photon-exchange approximation is good (this has been cross-checked), apply radiative corrections, and extract the structure functions νW_2 and W_1 (and W_3 for ν scattering). Scaling then implies that the structure functions are independent of any variables other than $x = -q^2/2m\nu$. However Eq (5) with N = 4 can be checked directly. Examining directly the dependence of $E\, d\sigma/d^3p$ on $p_\perp$ for fixed ratios of invariants would be most interesting. Even though radiative corrections (and possibly strong interactions in the hadronic wave function) surely generate logarithmic modifications of perfect scaling, such an analyses would provide a useful direct test of scaling.

Of course we find the parton model result that $pp \to \mu^+\mu^- + X$ or $\pi p \to \mu^+\mu^- + X$ can go via $q\bar{q} \to \mu^+\mu^-$ and hence is scale invariant. Similarly if the parton version of e^+e^- annihilation is taken, that it goes via $e^+e^- \to q\bar{q} \to$ hadrons, these counting rules give a scale invariant minimal scattering and hence $\sigma^{e^+e^-}_{Tot} \sim \frac{1}{s}$.

V. Summary and Conclusions

In this paper we have examined the conditions under which the simple dimensional analysis used to derive Eq. (1) can be valid in renormalizable field theories. The scaling laws are consistent with finite Bethe-Salpeter hadronic wavefunctions and the scaling behavior of simple planar Born diagrams for the n-particle scattering amplitude. The question of the short distance regularity of the Bethe-Salpeter wavefunction has now been partially settled for asymptotic freedom theories by Appelquist and Poggio[13]. They show, as conjectured in Ref. (1) that the irreducible kernel is more convergent in the ultraviolet than indicated by simple ladder approximation. We have given arguments why such behavior can be expected even in abelian theories, and why infrared corrections to the scaling laws are likely to be unimportant for color singlet or "neutral" hadronic states.

In a general renormalizable perturbation theory, the scaling laws can be violated by non-planar diagrams involving multiple on-shell quark-quark scattering. The fact that such diagrams do not seem to be important empirically, together with the absence of scale-invariant large transverse momentum inclusive reactions, plus the fact that effective Regge trajectories α_{eff} become negative at large t, evidently imply the suppression of scale-invariant (single or multiple) gluon exchange interactions between quarks of the scattering hadrons. This remarkable empirical fact has yet to be explained but undoubtedly has important implications for the detailed structure of the underlying quark theory.

Our general approach is different from what has been done previously. Starting with Wu and Yang, a number of authors have observed that given the asymptotic falloff of the hadronic form factors, predictions can be made about the large s and t behavior of elastic scattering[48]. Horn and Moshe[49] proposed that cross sections should have the form of Eq. (1), without specifying n, and showed that it provides a good fit to the data. In contrast, we look directly at the underlying short distance structure which we abstract from perturbation theory. This enables us to predict the behavior of the form factor (and automatically gives the relations between form factor and wide angle scattering obtained by previous authors)[48,50]. On the other hand, without making more detailed dynamical assumptions we cannot make the predictions that they make on the angular behavior of $2 \to 2$ scattering. The next logical step is to choose a theory which may actually be correct (e.g., a color gauge theory) and see whether qualitative features such as the angular dependence, the minimal high $p_\perp$ part of an inclusive scattering, etc., can be obtained without actually solving the theory. The techniques used in this paper, especially the simplified approach to bound state scattering which circumvents the complexities of the full Bethe-Salpeter analyses, should be very useful toward this goal.

In summary, the dimensional scaling laws for fixed angle scattering as $s \to \infty$

$$\frac{d\sigma}{dt}\,(A+B \to C+D) \to s^{2-n_A-n_B-n_C-n_D}\, f_{AB\to CD}\,(t/s),$$

give a fundamental connection between the degree of complexity of hadrons and the power law behavior of cross sections and form factors. Although much more experimental information is required, the present results support a composite representation of the hadrons based on quark degrees of freedom. Thus hadron scattering at large transverse momenta implies something of fundamental importance: Quarks not only have a mathematical existence, giving current algebra, Bjorken scaling, and the hadron spectrum, but a dynamical existence as well. That is not to say that quarks must be observed as free particles. However, bound state models should be built from quarks to incorporate the correct short distance structure of hadrons.

Acknowledgments

We have benefitted from conversations with many colleagues at SLAC and Caltech and elsewhere, especially T. Appelquist, J. D. Bjorken, R. Blankenbecler, J. Bronzan, P. Cvitanović, S. D. Drell, R. P. Feynman, Y. Frishman, M. Gell-Mann, J. Gunion, J. Kiskis, R. Sugar and T.-M. Yan.

Appendix A

Double-Scattering Graphs Using the Infinite-Momentum Method

The physics of the Landshoff multiple-scattering diagrams turns out to be particularly transparent using time-ordered perturbation theory in the infinite momentum frame. A full description of this method may be found in Ref. 51.

The prototype calculation which most simply contains the Landshoff contribution is given in the case of π-π scattering where we take a $f\phi^4$ theory for the constituents and $g\phi^3$ vertices to represent the bound states. Generalizations to other cases will be straightforward.

We choose the following reference frame

$$p = p_B = \left(P + \frac{M_B^2}{4P} , \vec{0}_\perp , P - \frac{M_B^2}{4P}\right)$$

$$p_D = p_B + q, \quad p_C = p_B + r, \quad p_A = p_B + q + r$$

with

$$q = \left(\frac{q \cdot p}{2P} , \vec{q}_\perp , - \frac{q \cdot p}{2P}\right)$$

$$r = \left(\frac{r \cdot p}{2P} , \vec{r}_\perp , - \frac{r \cdot p}{2P}\right) .$$

Note that $t = q^2 = - \vec{q}_\perp^{\,2}$, and $u = r^2 = - \vec{r}_\perp^{\,2}$.

We also have $\vec{q}_\perp \cdot \vec{r}_\perp = 0$ if $M_A^2 + M_B^2 = M_C^2 + M_D^2$.

The contributing time-ordered diagrams which are equivalent to the Feynman graph, Fig. 21a, are shown in Fig. 21b-e. All other time-orderings vanish in the $P \to \infty$ frame. It is easy to check that diagrams (d) and (e) do not contribute to leading order in the asymptotic fixed angle limit. Diagrams (b) and (c) include the summation over time-orderings in which the vertex A occurs before and after B, and C occurs before and after D. The total amplitude for M(b) and M(c) is then given by the following three-loop expression from time-ordered perturbation theory:

$$M = \int \prod_{i=1}^{4} \left[\frac{d^2k_i\, dx_i}{2x_i(1-x_i)(2\pi)^3} \right] \delta(x_a+x_b-x_c-x_d)$$

$$\delta^{(2)}(\vec{k}_{\perp b}+\vec{k}_{\perp a}+x_a(\vec{q}+\vec{r}) - \vec{k}_{\perp c} - x_c\vec{r} - \vec{k}_{\perp d} - x_a\,\vec{q})$$

$$\psi_A(\vec{k}_{\perp a},x_a)\psi_B(\vec{k}_{\perp b},x_b)\psi_C(\vec{k}_{\perp c},x_c)\psi_D(\vec{k}_{\perp d},x_d)$$

$$M_{(1)}\; M_{(2)} \left[\frac{1}{D_{(b)}} + \frac{1}{D_{(c)}} \right] . \tag{A1}$$

Three momentum is conserved at each vertex. The range of the x_i is 0 to 1. The amplitudes $M_{(1)}$ and $M_{(2)}$ are the scattering amplitudes for $a + b \to c + d$ and $a' + b' \to c' + d'$, respectively. In the $f\phi^4$ theory $M_{(1)} = M_{(2)} = f$. The energy denominators for diagrams (b) and (c) are

$$D_{(b)} = E_A + E_B - E_c - E_{a'} - E_d - E_{b'} + i\varepsilon$$

$$D_{(c)} = E_A + E_B - E_{c'} - E_a - E_{d'} - E_b + i\varepsilon$$

where the E_i are the relativistic "kinetic energies"

$$E_i = \frac{\vec{k}_{\perp i}^2 + m_i^2}{x_i} ,$$

e.g., $E_a = [(\vec{k}_{\perp a} + x_a(\vec{q}+\vec{r}))^2 + m_a^2]/x_a$.

In addition there are two energy denominators coming before the scatterings M_1 and M_2 and two afterward. When these are summed over the orderings A before and after B, C before and after D, they generate the product of wavefunctions:

$$\psi_A(k_{\perp a},x_a) = \frac{g}{M_A^2 - \frac{k_{\perp a}^2+m_a^2}{x_a} - \frac{k_{\perp a}^2+m_{a'}^2}{1-x_a}} ,$$

etc. Notice that because of the choice of variables ($\vec{p}_a = x_a\ (\vec{p}+\vec{q}+\vec{r}) + \vec{k}_{\perp a}$) the wavefunctions do not depend explicitly on q or r. The natural domain of the wavefunction is thus $\vec{k}_{\perp a}$ finite.

Dropping terms of order M^2 temporarily we have

$$D_{(b)} \cong (\vec{q}+\vec{r})^2 - x_c\vec{r}_\perp^{\,2} - (1-x_a)(\vec{q}+\vec{r})^2 - x_d\vec{q}^{\,2}$$

$$- \vec{k}_{\perp c}\cdot\vec{r} + 2\vec{k}_{\perp a}\cdot(\vec{q}+\vec{r}) - 2\vec{k}_{\perp d}\cdot\vec{q}$$

$$- \frac{\vec{k}_{\perp c}^{\,2}}{x_c} - \frac{\vec{k}_{\perp a}^{\,2}}{1-x_a} - \frac{\vec{k}_{\perp d}^{\,2}}{x_d} - \frac{\vec{k}_{\perp b}^{\,2}}{1-x_b} \quad .$$

If we introduce the scaled variables

$$\alpha m \equiv (x_a-x_d)|\vec{q}| + 2(\vec{k}_{\perp a}-\vec{k}_{\perp d})\cdot\hat{q}$$

$$\beta m \equiv (x_a-x_c)|\vec{r}| + 2(\vec{k}_{\perp a}-\vec{k}_{\perp d})\cdot\hat{r} \quad ,$$

then for α and β of order 1 and $k_{\perp a}^2$, $k_{\perp b}^2$ and $k_{\perp c}^2$ of order m^2, we have

$$\vec{k}_{\perp b}^{\,2} \sim O(m^2)$$

and

$$D_{(b)} = \alpha|\vec{q}| + \beta|\vec{r}| + O(m) + i\varepsilon \quad .$$

Changing variables from x_d and x_c to α and β thus gives for diagram (b)

$$M_{(b)} \sim \frac{1}{m|\vec{q}||\vec{r}|}\int\frac{d\alpha d\beta}{\alpha|\vec{q}| + \beta|\vec{r}| + O(m) + i\varepsilon} \tag{A2}$$

multiplied by a finite integral over dx_a, $d^2k_{\perp a}$, $d^2k_{\perp c}$, $d^2k_{\perp d}$ which is independent of s, t and u. The imaginary part of (A2) gives

$$M_{(b)} \sim \frac{i}{m\sqrt{stu}} \tag{A3}$$

(as easily seen in polar coordinates) and the real part cancels against $M_{(c)}$.

We should note the following at this point. The π-π amplitude is imaginary, reflecting the Glauber-like real pole intermediate states which contribute. The constituent scattering amplitudes $M_{(1)}$ and $M_{(2)}$ in (A3) correspond to near-mass-shell scatterings of the constituents of different hadrons with fractional momenta x_a and $1-x_a$, respectively. Note that the wavefunction dependence is not relevant as long as the $d^2k_\perp$ integrals converge because if the $M_i(x)$ are scale invariant they are actually independent of x, e.g., for vector gluon exchange $M(x) \sim \frac{xs-xu}{xt} = \frac{s-u}{t}$. The generalization to more realistic scatterings is immediate. Each additional pair beyond the first two gives a factor in the amplitude of order

$$\frac{1}{m\sqrt{stu}} ,$$

thus giving the result, Eq. (21) of Section II.B1.

Appendix B

Fixed Angle Unitarity

It is interesting that the behavior

$$|M_n|^2 \sim s^{4-n} \tag{B1}$$

is actually the fixed angle unitarity bound for n particles in the external state when the square of the amplitude is averaged over a fixed angular region in the center of mass. A convenient proof has been given by Bardeen[52] as follows: Consider a two-particle state with continuum normalization

$$\langle 2|2'\rangle_{cm} = 2E_a\,\delta^3(\vec{p}_a-\vec{p}_a{}')\,2E_b\,\delta^3(\vec{p}_b-\vec{p}_b{}')$$

$$= \frac{4\sqrt{s}}{p_{cm}}\,\delta(\Omega-\Omega')\,\delta^4(p_a+p_b-p_a{}'-p_b{}')\ .$$

By smearing with an angular function

$$|\bar{2}\rangle = \int |2\rangle d\Omega\, f(\Omega), \qquad \int |f(\Omega)|^2 d\Omega = 1$$

we have

$$\langle\bar{2}|\bar{2}'\rangle = \frac{4\sqrt{s}}{p_{cm}}\,\delta^4(p_a+p_b-p_a{}'-p_b{}')\ .$$

Unitarity then gives

$$\langle\bar{2}|\bar{2}'\rangle = \langle\bar{2}|S^\dagger S|\bar{2}'\rangle = \sum_N \int \langle\bar{2}|S^\dagger|N\rangle \prod_{i=1}^{N} \frac{d^3p_i}{2\omega_i}\,\langle N|S|\bar{2}'\rangle$$

and hence

$$\frac{4\sqrt{s}}{p_{cm}} = \sum_N \int |\langle\bar{2}|T|N\rangle|^2 \prod_{i=1}^{N} \frac{d^3p_i}{2\omega_i}\,(2\pi)^8\,\delta^4(p_a+p_b-\sum_{i=1}^{N} p_n)\ .$$

Averaging $|N\rangle$ over cm angles thus gives in the high energy limit

$$\int d\Omega\,|\langle\bar{2}|T|N\rangle|^2 \leq C_N\, s^{2-N}$$

where N is the number of particles in the final state. By crossing, the proof holds for any number of initial particles and (B1) follows.

The bound (B1) is also often imposed on amplitudes in each order of perturbation theory as a necessary condition for renormalizability.

In our work we show that the bound (B1) for the fixed angle amplitude is saturated in any theory without an inherent short distance scale. A crucial point must be noted, however. In the hadronic amplitude, the constituent particles for each hadron are not at fixed angles relative to each other; thus the bound (B1) for the required amplitude M_n can, in principle, fail due to singular behavior when the external lines become parallel. This is in fact what occurs in the multiscattering diagram considered by Landshoff. (See Sec. II.B1 and Appendix A.)

Footnotes and References

1. A brief description of the results of this article were given in S. J. Brodsky and G. R. Farrar, Phys. Rev. Lett. 31, 1153 (1973).
2. V. Matveev, R. Muradyan and A. Tavkhelidze, Lett. Nuovo Cim. 7, 719 (1973).
3. The initial application of this result for antiquark distributions was given by G. R. Farrar, to be published Nuc. Phys. B77. The general result (Eq. (6)) and further applications are discussed by R. Blankenbecler and S. J. Brodsky, SLAC-PUB-1430 and J. Gunion, Univ. of Pittsburgh preprint, PITT-122.
4. Z. F. Ezawa, Cambridge preprint DAMTP 74/5.
5. See, for instance, J. Harte, Phys. Rev. 165, 1157 (1968) and 171, 1825 (1968).
6. E. E. Salpeter and H. A. Bethe, Phys. Rev. 84, 1232 (1951). A complete discussion of scattering amplitudes in the Bethe-Salpeter formalism is given by S. Mandelstam, Proc. Roy. Soc. (London) A233, 248 (1953).
7. P. V. Landshoff, Cambridge preprint, DAMTP 73/36, to be published.
8. P. V. Landshoff and J. C. Polkinghorne, Phys. Lett. 44B, 293 (1973).
9. A similar analysis has been given recently by Ezawa, Ref. 4, and C. Alabiso and G. Schierholz, to be published Phys. Rev. D, August 1974.
10. See, e.g., E. E. Salpeter, Phys. Rev. 87, 328 (1952).
11. A useful trick to perform the calculation is to make use of the identity $\sum_{\pm s} u(k,s)\bar{v}(k,-s) = (\not{k} + m)\gamma_5$ and its generalizations to unequal momenta. The expression for M_5^μ is then seen to be just an ordinary trace of γ-matrices.
12. For a review see S. J. Brodsky, Comments in Atomic and Molecular Physics.
13. T. Appelquist and E. Poggio, Harvard preprint.
14. We are indebted to L. Caneschi and M. Gell-Mann for raising the question of the effect of orbital angular momentum on the scaling laws.
15. M. Ciafaloni, Phys. Rev. 176, 1898 (1968).
16. In addition a very elegant Feynman parameter calculation has been performed by P. Cvitanović, SLAC-PUB-1409.

17. It can be shown using the Coleman-Norton rules, Phys. Rev. 125, 1422 (1962), that the only infrared linearly divergent diagrams are of the Landshoff type. S. Coleman, private communication.

18. The prediction of the Landshoff diagrams for $pp \to pp$ and a number of other processes which are measurable have been obtained in a colored quark and vector gluon theory by G. R. Farrar and C.-C. Wu, Caltech preprint CALT-68-455. They verify that for this, as well as other renormalizable theories, there is no "accidental" cancellation of these leading diagrams. Comparing the angular dependence of $pp \to pp$ implied by the Landshoff model with the data, they find that it provides considerably more convincing evidence against the existence of such a process than the power falloff alone.

19. J. C. Polkinghorne, Phys. Lett. 49B, 277 (1974).

20. T. Appelquist and E. Poggio, private communication and ref. 13.

21. R. Blankenbecler, S. J. Brodsky and J. F. Gunion, Phys. Lett. 39B, 649 (1972) and Phys. Rev. D8, 187 (1973).

22. H. Fritzsch and M. Gell-Mann, Proc. of the XVI Intl. Conf. on High Energy Physics, The Univ. of Chicago and NAL, 1972, Vol. 2.

23. We use the notation of Bjorken and Drell: $\langle p+q | J_\mu(0) | p \rangle = \bar{u}(p+q)[\gamma_\mu F_1(q^2) + \frac{\sigma_{\mu\nu} q^\nu}{2M} \kappa F_2(q^2)] u(p)$, where κ is the anomalous magnetic moment. The commonly used "electric" and "magnetic" form factors are related to F_1 and F_2 by $G_E(q^2) = F_1(q^2) + \frac{\kappa q^2}{4M^2} F_2(q^2)$ and $G_M(q^2) = F_1(q^2) + \kappa F_2(q^2)$.

24. We thank G. C. Fox for a helpful discussion on this point. It has been pointed out by J. Gunion that in simple Born diagrams there may be additional t dependence.

25. This provides a somewhat more general derivation of the α_{eff} than was obtained by direct calculation in the interchange model, however the physics is the same. The results agree except for $\alpha_{eff}^{pp\to pp}$ which differs due to the fact that the original interchange model assumed a "quark-core" representation for the proton which led to the prediction $d\sigma/dt\ (pp \to pp) \sim s^{-12}$ rather than the dimensional scaling s^{-10}.

26. R. Blankenbecler, D. Coon, J. Gunion and T. Than-Van, SLAC preprint in preparation.

27. D. R. Yennie, S. C. Frautschi and H. Suura, Annals of Physics 13, 379 (1961) and N. Meister and D. R. Yennie, Phys. Rev. 130, 1210 (1963), and references therein.

28. This is natural for models which aim to unify strong, weak, and electromagnetic interactions and has been especially emphasized by H. Fritzsch and P. Minkowski, Phys. Lett. 49B, 462 (1974) and by H. D. Politzer, Phys. Rev. D9, 2174 (1974).

29. S. Weinberg, Phys. Rev. 140B, 516 (1965).

30. The summation of leading logarithms in the infrared-protected pseudoscalar theory gives a correction of order $[\log t]^{3/10}$ to the fermion form factor; see T. Appelquist and J. R. Primack, Phys. Rev. D1, 1144 (1970) and references therein. We would like to thank T.-M. Yan and P. Cvitanović for helpful conversations on the infrared problem.

31. For instance A. De Rujula, Phys. Rev. Lett. 32, 1143 (1974) and D. Gross and S. B. Treiman, Phys. Rev. Lett. 32, 1145 (1974) have an indirect argument that the logarithmic modifications of perfect scaling for the proton form factor (Eq. (2)) should be of the rather mild form $(\ln q^2)^{\ln q^2}$.

32. R. Madaras et al., Phys. Rev. Lett. 30, 507 (1973) and H. Newman et al., Phys. Rev. Lett. 32, 483 (1974).

33. Talk presented by A. Boyarski at the Washington APS Meeting, April 1974 and B. L. Beron et al., Stanford preprint HEPL No. 734.

34. P. N. Kirk et al., Phys. Rev. D8, 63 (1973).

35. J. Litt et al., Phys. Lett. 31B, 40 (1970).

36. J. S. Ball and F. Zachariasen, Phys. Rev. 170, 1541 (1968);
D. Amati, R. Jengo, H. Rubenstein, G. Veneziano and M. Virasoro, Phys. Lett. 27B, 38 (1968);

D. Amati, L. Caneschi and R. Jengo, Nuovo Cimento 58A, 783 (1968);

M. Ciafaloni and D. Menotti, Phys. Rev. 173, 1575 (1968);

S. D. Drell and T. D. Lee, Phys. Rev. D5, 1738 (1972).

37. We wish to thank W. Atwood for a discussion of this point.

38. M. Bernardini et al., Phys. Lett. 46B, 261 (1973).

39. There is already evidence that this may be the case from photoproduction off nuclei which shows less shadowing than expected from pure vector dominance. See, e.g., K. Gottfried, Proc. of the 1971 Intl. Symposium on Electron and Photon Interactions at High Energies, Cornell, N.Y.

40. R. L. Anderson et al., Phys. Rev. Lett. 30, 627 (1973).

41. V. Chaband et al., Phys. Lett. 38B, 441 (1972).

42. G. W. Brandenburg et al., Phys. Lett. 44B, 305 (1973).

43. Recently data on $p\bar{p} \rightarrow p\bar{p}$ at P_{lab} = 5 and 6.2 GeV/c have been obtained by T. Buran et al., CERN preprint, however the errors are so large that it is consistent with both a constant and s^{-10} falloff.

44. Most of these results need little explanation beyond what was given in Ref. 1 so this analysis will be brief and principally for completeness. For a detailed review of recent developments, experimental and theoretical, see R. Blankenbecler and S. J. Brodsky, SLAC-PUB-1430 and R. Blankenbecler, SLAC-PUB-1438.

45. S. Berman, J. D. Bjorken and J. Kogut, Phys. Rev. D4, 2381 (1971).

46. R. Blankenbecler, S. J. Brodsky and J. Gunion, Phys. Lett. 42B, 461 (1972).

47. F. W. Büsser et al., Phys. Lett. 46B, 471 (1973);

J. W. Cronin et al., Phys. Rev. Lett. 31, 1426 (1973). See also "Large Transverse Momentum Phenomena," report of an ISR discussion meeting, for further relevant experiments.

48. T. T. Wu and C. N. Yang, Phys. Rev. 137B, 708 (1965);

H. D. I. Abarbanel, S. D. Drell and F. J. Gilman, Phys. Rev. Lett. 20, 280 (1968);

T. K. Gaisser, Phys. Rev. D3, 1337 (1970) and Ref. 21, among others.

49. D. Horn and M. Moshe, Nuc. Phys. B48, 557 (1972) and Nuc. Phys. B57, 139 (1973).

50. W. R. Theis, Nucl. Phys. Ltrs. 42B, 246 (1972) gives a connection between form factors and wide angle scattering by assigning "anomalous dimensions" to the hadron fields. However, since all the hadrons are not probed at short distances or on the light cone a consistent analysis of this type does not seem possible.

51. J. D. Bjorken, J. Kogut and D. Soper, Phys. Rev. D3, 1382 (1970) and S. Brodsky, R. Roskies and R. Suaya, Phys. Rev. D, to be published.

52. W. Bardeen, private communication.

Figure Captions

1. n-point "decomposition" of AB $\rightarrow$ CD (in this example n = 10).
2. Schematic representation of the full meson-meson scattering amplitude in terms of Bethe-Salpeter wave functions ψ and the irreducible amplitude M_n.
3. Example of a disconnected or non-planar diagram for pp $\rightarrow$ pp wide angle scattering.
4. Schematic representation of the Bethe-Salpeter equation for a two-particle bound state.
5. The meson form factor in ladder approximation to the Bethe-Salpeter equation.
6. Examples of non-ladder kernels for the Bethe-Salpeter equation and the irreducible contributions to the current matrix element they engender by gauge invariance.
7. Born diagram (5 point connected amplitude M_5^μ) for the meson form factor.
8. Schematic representation of the Bethe-Salpeter equation for a three-particle bound state.
9. Diagram for meson baryon scattering with multiple scattering of near-mass-shell quarks of different hadrons.
10. Typical Born diagrams for meson-baryon scattering via (a) gluon exchange and (b) quark exchange. The dots label quark lines which are far off mass shell. All gluons shown are far off mass shell.
11. The pinch in meson-meson scattering (a) Feynman graph and (b) momentum space picture of the scatterings.
12. Born diagram for photoproduction. The heavy dots represent far off shell quark lines. All gluon lines shown are far off shell.
13. Typical Born diagrams for baryon form factors.
14. Hadron scattering for t large, s $\rightarrow \infty$ if (a) gluon exchange or (b) quark interchange is dominant in the t channel.

15. $(q^2)^2 G_M(q^2)/\mu$ for the proton versus $-q^2$; data from P. N. Kirk et al.[34]

16. $q^2 F_\pi(q^2)$ for the pion versus q^2; data from M. Bernardini et al.[38]

17. $d\sigma/d\Omega$ (90° c.m.) versus s for several meson-baryon scattering reactions. This figure is from Ref. 42.

18. Log $(d\sigma/dt)$ for $pp \to pp$ versus log s at various c.m. angles. Only data for $s > 15\ \mathrm{GeV}^2$ and $|t| > 2.5\ \mathrm{GeV}^2$ are included. This figure is from Ref. 8.

19. Parton model picture for (a) the one-photon-exchange deep inelastic scattering and (b) the colored gluon exchange contribution to high $p_\perp$ inclusive scattering, showing the color index i(j) of the quarks. The notation -i(-j) refers to the color of the rest of the hadron.

20. Possible minimal large $p_\perp$ scatterings if gluon exchange is not allowed: (a) $q''\pi'' \to q\pi$ and (b) $qq \to \pi qq$.

21. (a) A Feynman diagram for $\pi\pi \to \pi\pi$ and (b)-(e) time-ordered diagrams corresponding to it.

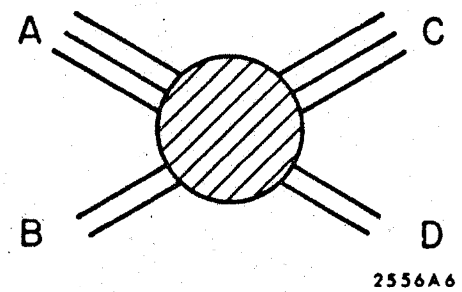

Fig. 1

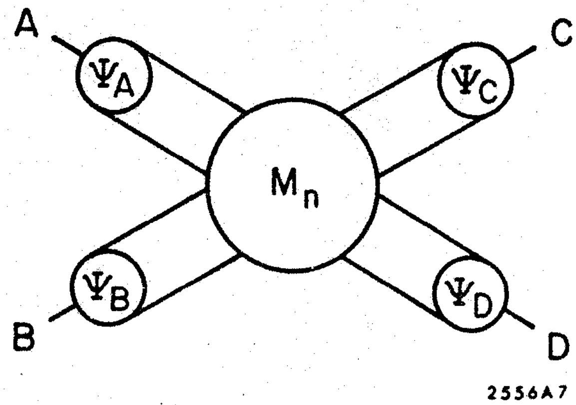

Fig. 2

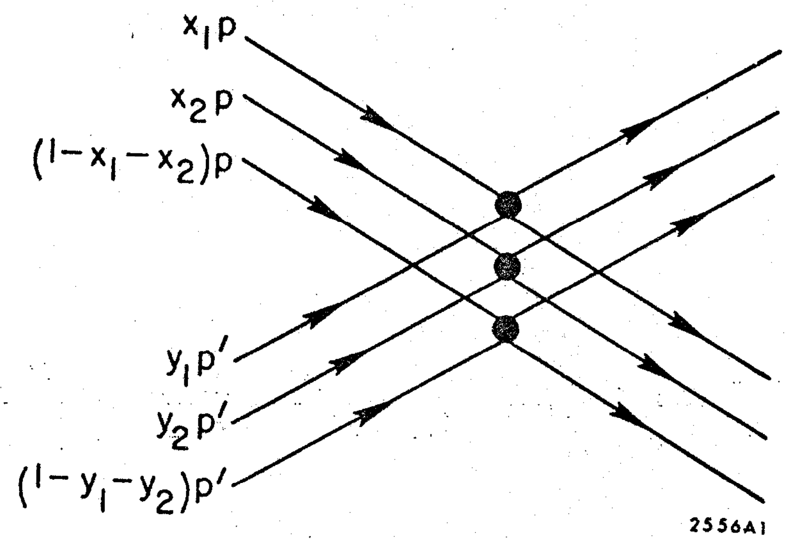

Fig. 3

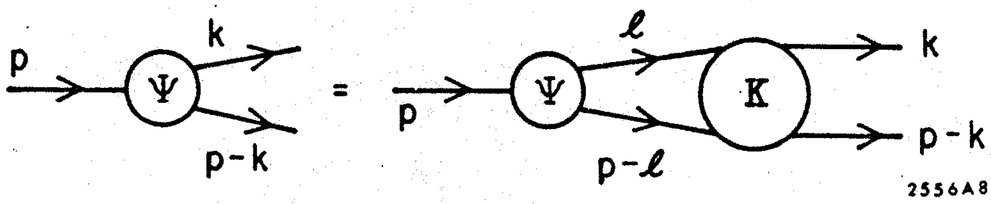

Fig. 4

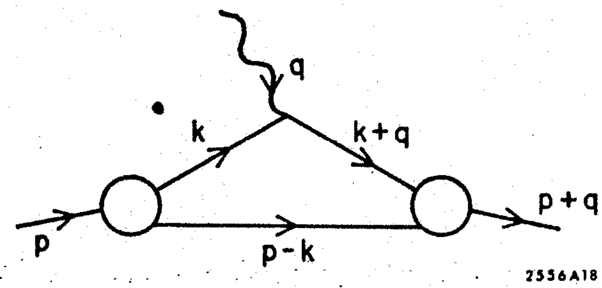

Fig. 5

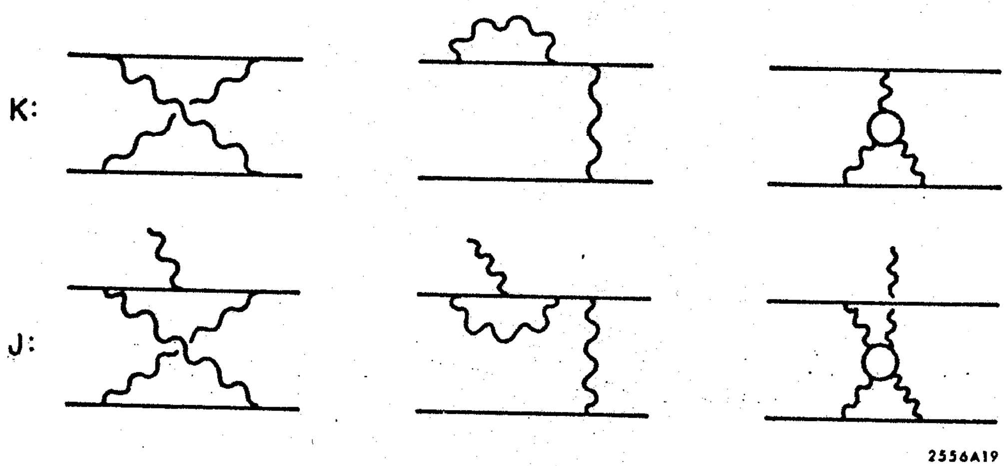

Fig. 6

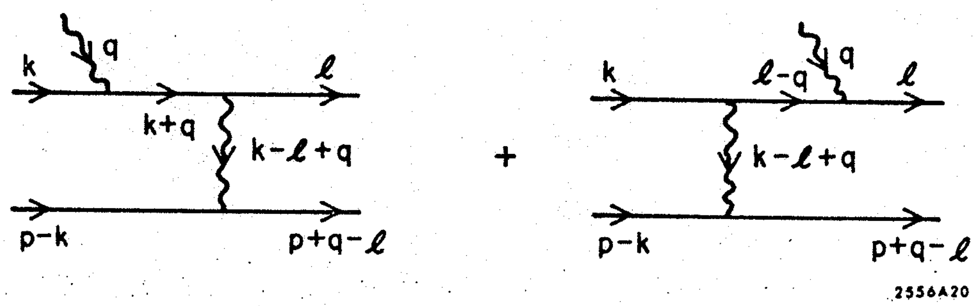

Fig. 7

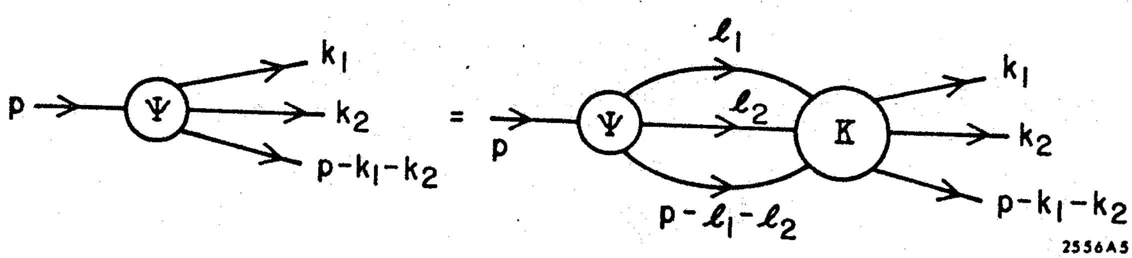

Fig. 8

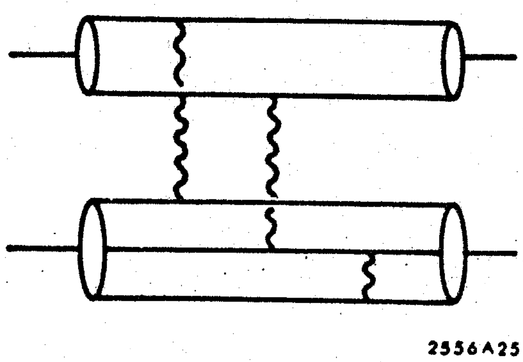

Fig. 9

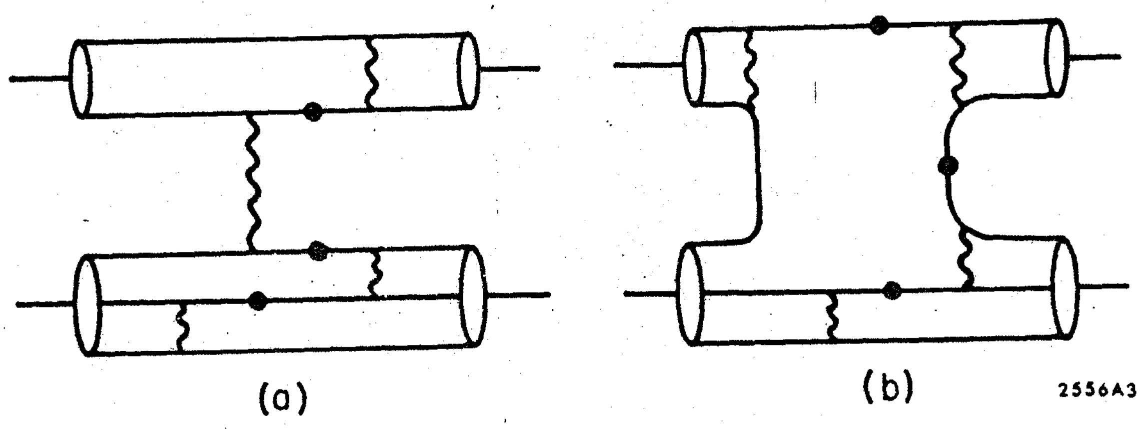

(a)
(b)
2556A3

Fig. 10

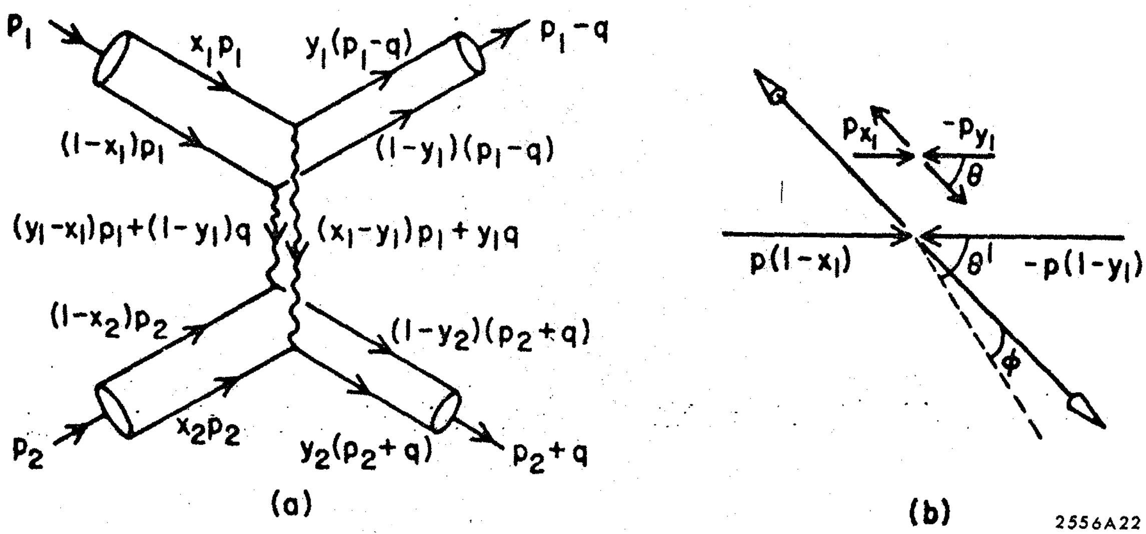

p_1
$x_1 p_1$
$y_1(p_1-q)$
p_1-q
$(1-x_1)p_1$
$(1-y_1)(p_1-q)$
$(y_1-x_1)p_1+(1-y_1)q$
$(x_1-y_1)p_1+y_1 q$
$(1-x_2)p_2$
$(1-y_2)(p_2+q)$
p_2
$x_2 p_2$
$y_2(p_2+q)$
p_2+q
(a)
p_{x_1}
$-p_{y_1}$
θ
$p(1-x_1)$
θ'
$-p(1-y_1)$
ϕ
(b)
2556A22

Fig. 11

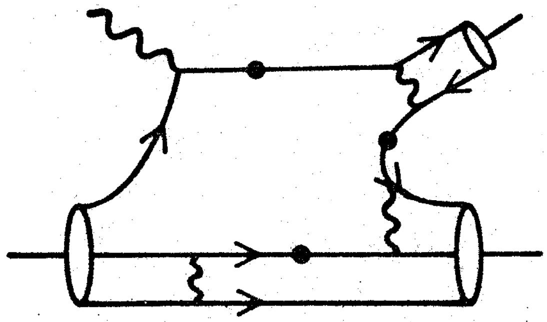

Fig. 12

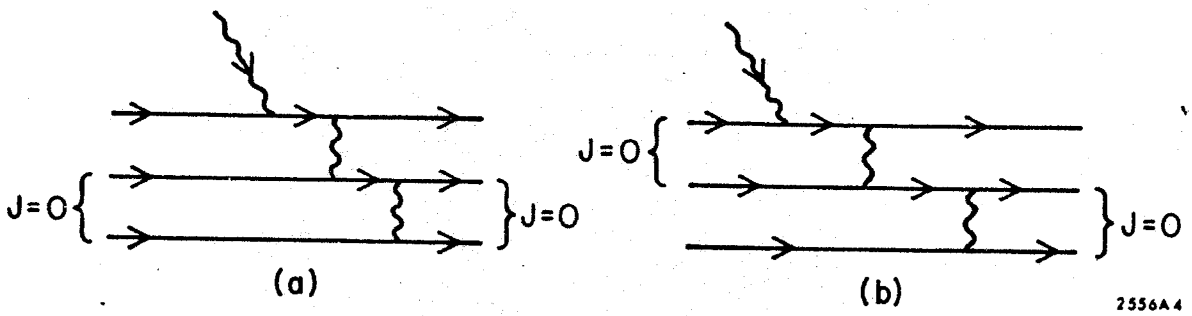

Fig. 13

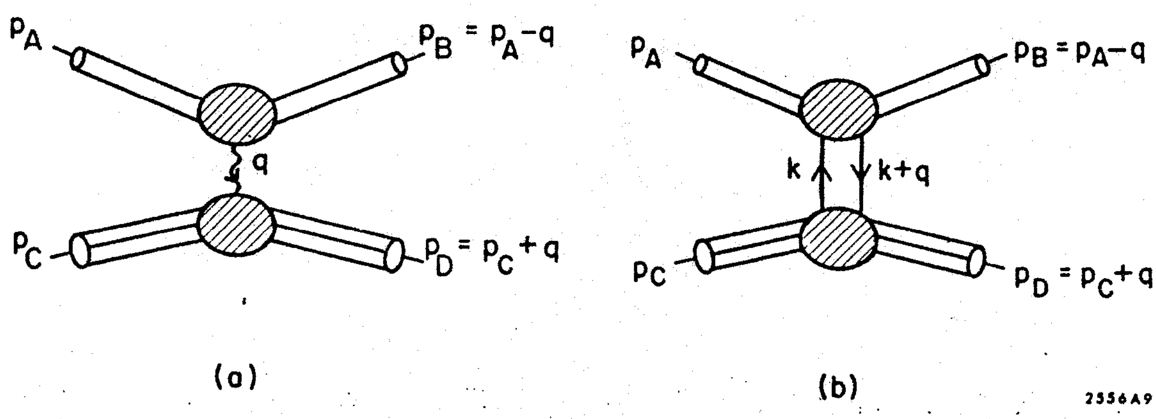

Fig. 14

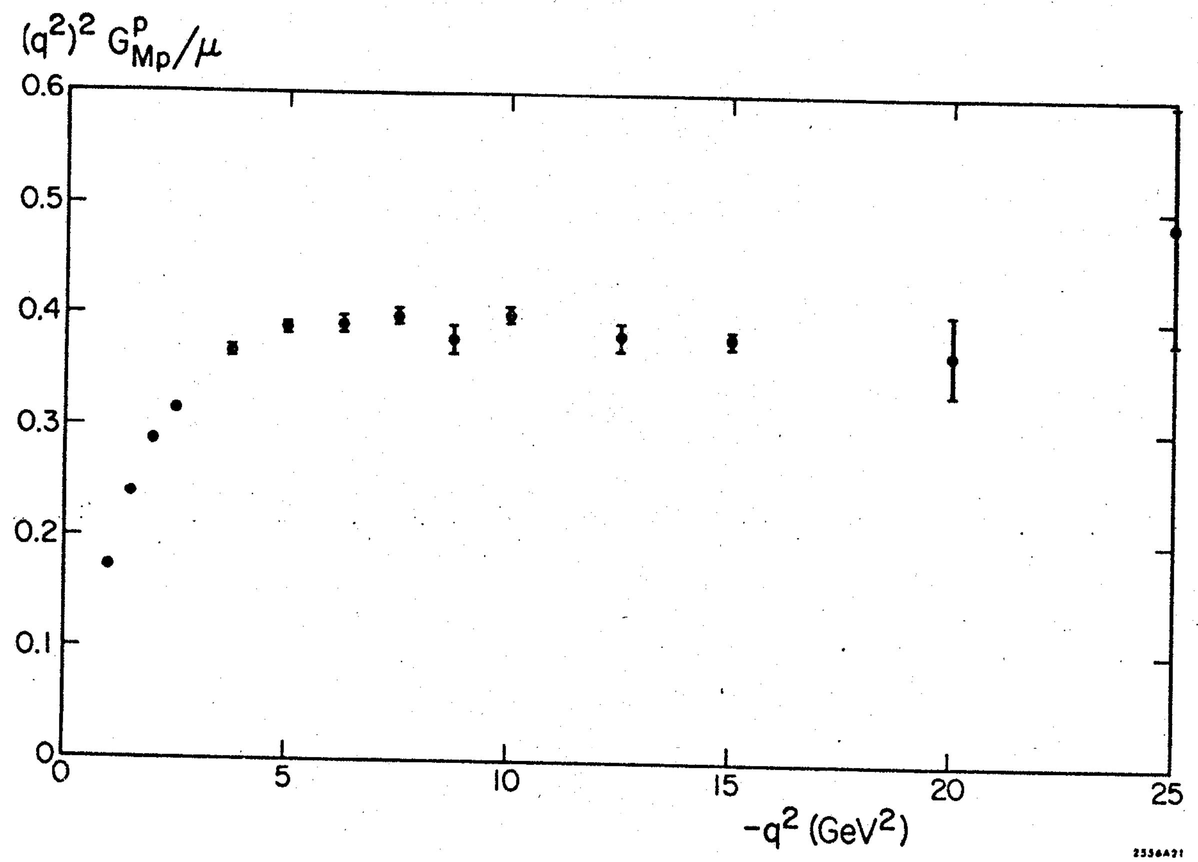

(q2)2 GpMp/μ
0.6
0.5
0.4
0.3
0.2
0.1
0
0
5
10
15
20
25
-q2 (GeV2)
2556A21

Fig. 15

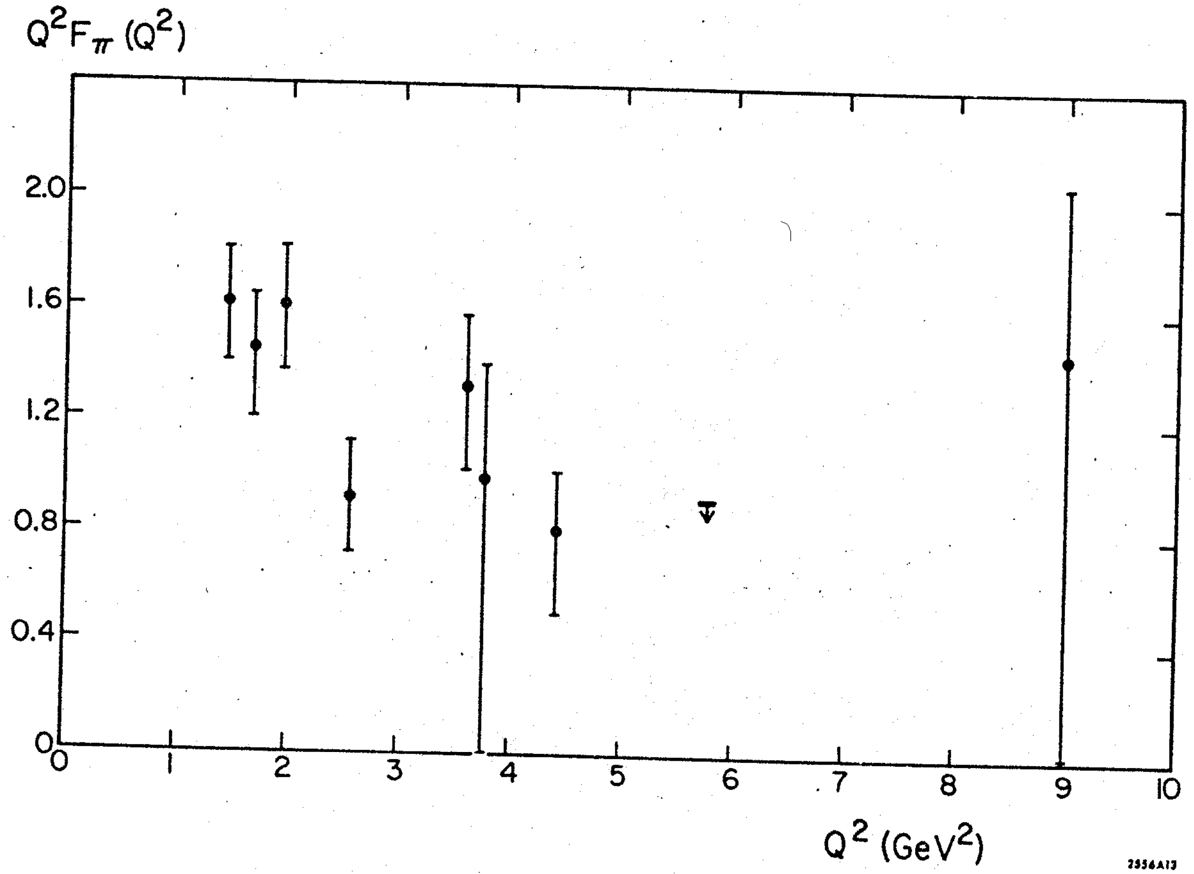

Q2Fπ (Q2)
2.0
1.6
1.2
0.8
0.4
0
0
1
2
3
4
5
6
7
8
9
10
Q2 (GeV2)
2556A13

Fig. 16

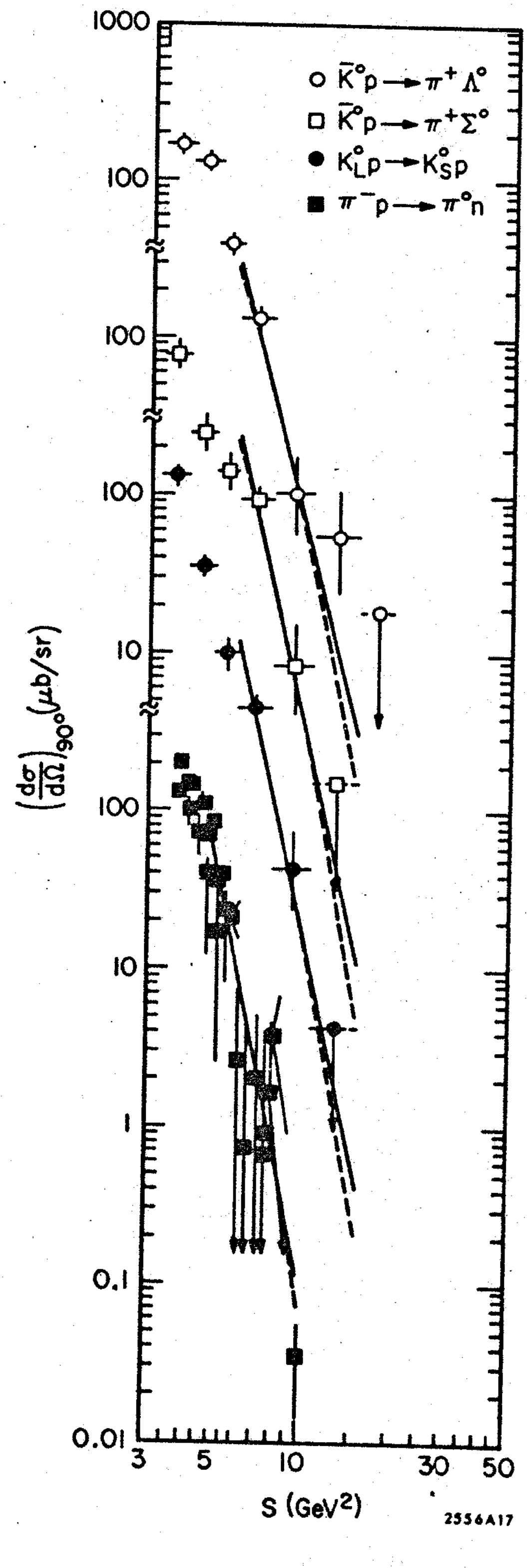

1000
100
100
100
10
100
10
1
0.1
0.01
3
5
10
30
50
$\bar{K}^\circ p \rightarrow \pi^+ \Lambda^\circ$
$\bar{K}^\circ p \rightarrow \pi^+ \Sigma^\circ$
$K^\circ_L p \rightarrow K^\circ_S p$
$\pi^- p \rightarrow \pi^\circ n$
$\left(\frac{d\sigma}{d\Omega}\right)_{90^\circ} (\mu b/sr)$
S (GeV^2)
2556A17

Fig. 17

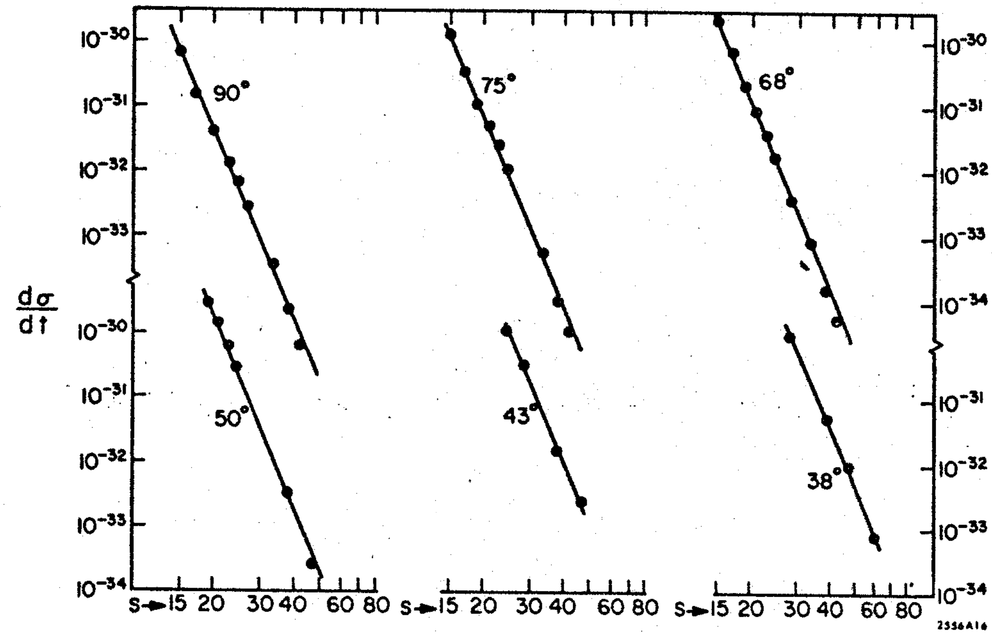

10^{-30}
10^{-31}
10^{-32}
10^{-33}
10^{-34}
$\frac{d\sigma}{dt}$
90°
75°
68°
50°
43°
38°
S→15 20 30 40 60 80
2556A16

Fig. 18

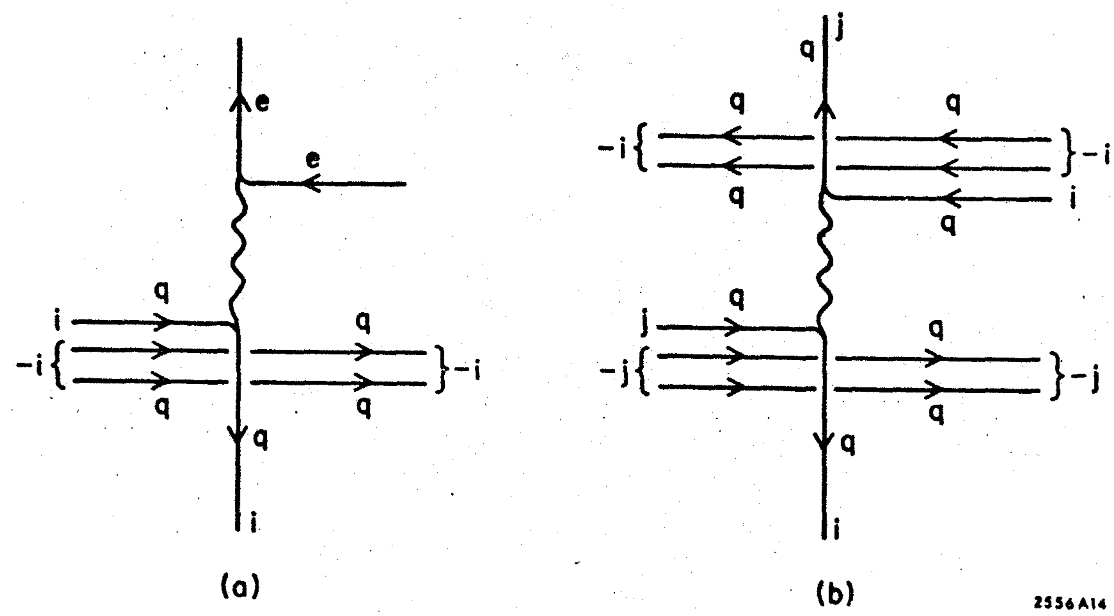

Fig. 19

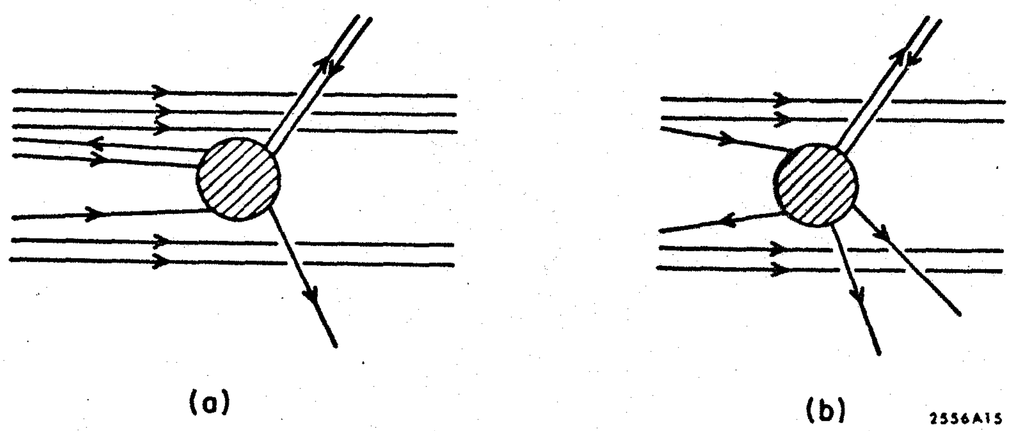

Fig. 20

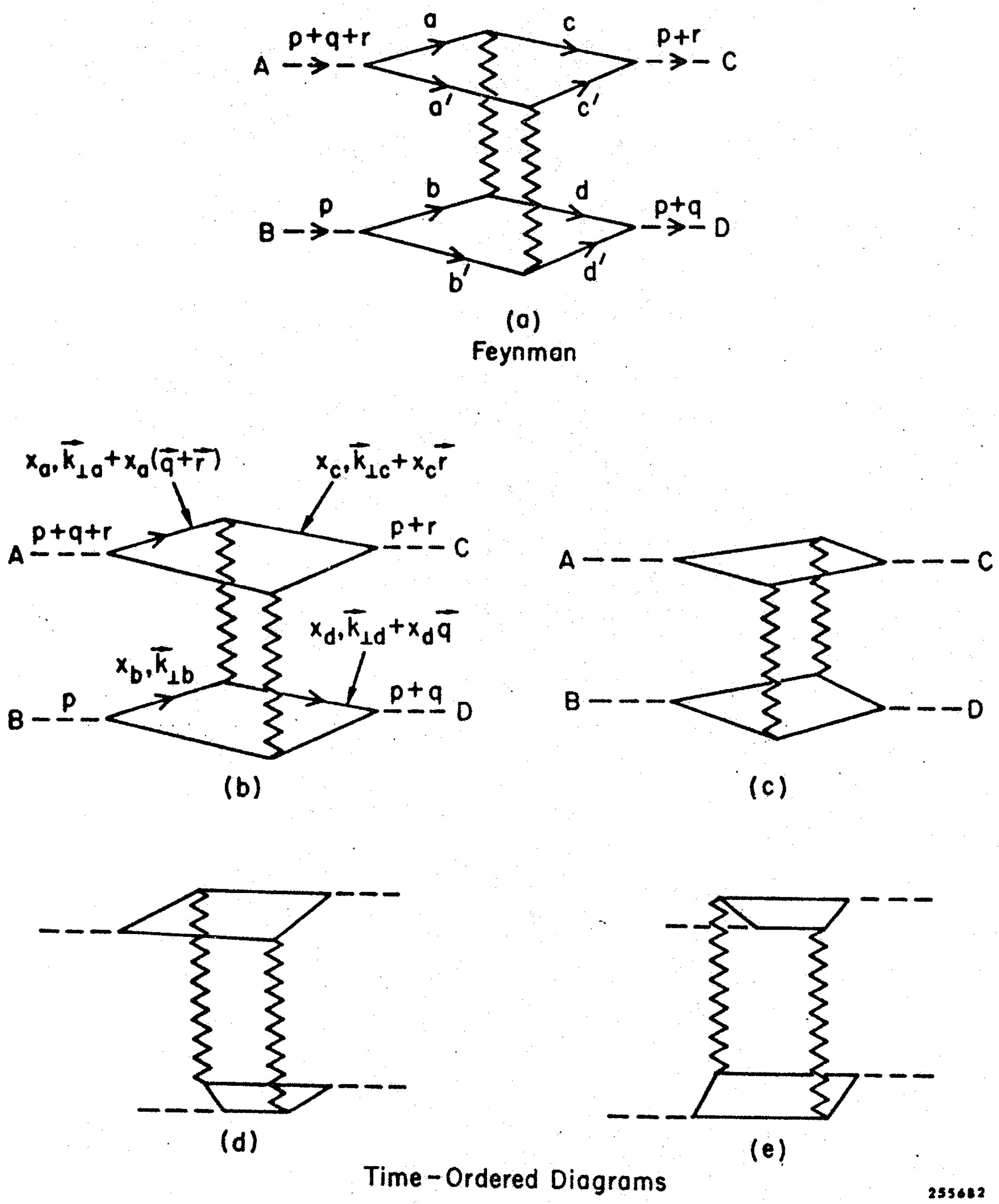
p+q+r
a
c
p+r
A
C
a'
c'
b
d
p
p+q
B
D
b'
d'
(a)
Feynman
$x_a, \vec{k}_{\perp a} + x_a(\vec{q}+\vec{r})$
$x_c, \vec{k}_{\perp c} + x_c\vec{r}$
$x_d, \vec{k}_{\perp d} + x_d\vec{q}$
$x_b, \vec{k}_{\perp b}$
(b)
(c)
(d)
(e)
Time-Ordered Diagrams
255682

Fig. 21